NEANDC (E) - 312 - U Vol. V
INDC (Ger) -035/LN+Special

PROGRESS REPORT ON NUCLEAR DATA RESEARCH IN THE FEDERAL REPUBLIC OF GERMANY

for the Period April 1, 1989 to March 31, 1990

June 1990

Edited by
S. Cierjacks
Kernforschungszentrum Karlsruhe
Institut für Material- und Festkörperforschung
Federal Republic of Germany

NEANDC(E)-312-U Vol. V
INDC(Ger)-35/LN+Special

PROGRESS REPORT ON NUCLEAR DATA RESEARCH IN THE FEDERAL REPUBLIC OF GERMANY

for the Period April 1, 1989 to March 31, 1990

June 1990

Edited by
S. Cierjacks
Kernforschungszentrum Karlsruhe
Institut für Material- und Festkörperforschung
Federal Republic of Germany

FOREWORD

This report has been prepared to promote the exchange of nuclear data research information between the Federal Republic of Germany and other member states of NEA and IAEA. It brings together progress reports from KfK Karlsruhe, KFA Jülich, GKSS Geesthacht, the universities of Hannover, Köln, Mainz, München and Stuttgart, as well as from PTB Braunschweig and FIZ Karlsruhe. As in previous years, the emphasis in the work reported here is on measurement, evaluation and compilation of application-oriented nuclear data, such as those relevant to fission and fusion reactor technologies, development of intense neutron sources, astrophysics research, cosmogenic and meteoritic investigations, production of medically important radioisotopes, etc.

Each contribution is presented under the laboratory heading where the work was done. When the work is relevant to requests in the World Request List for Nuclear Data, WRENDA 83/84 (INDC(SEC)-88/URSF), the corresponding request identification numbers are given in the headings of the respective contributions.

Karlsruhe, June 1990 S. Cierjacks

CONTENTS

Page

INSTITUT FÜR KERNPHYSIK, ARBEITSGRUPPE STRAHLUNGSTRANSPORT FORSCHUNGSZENTRUM JÜLICH

INSTITUT FÜR KERNPHYSIK, EXPERIMENTELLE KERNPHYSIK II FORSCHUNGSZENTRUM JÜLICH

KERNFORSCHUNGSZENTRUM KARLSRUHE
INSTITUT FÜR KERNPHYSIK III

1. CAPTURE CROSS SECTION MEASUREMENTS OF Xe AND Kr ISOTOPES BY FAST CYCLIC ACTIVATION

H. Beer

The measurement of particular isotopic capture cross sections of Kr and Xe is made difficult because of the high costs for separate isotopes. In this situation the

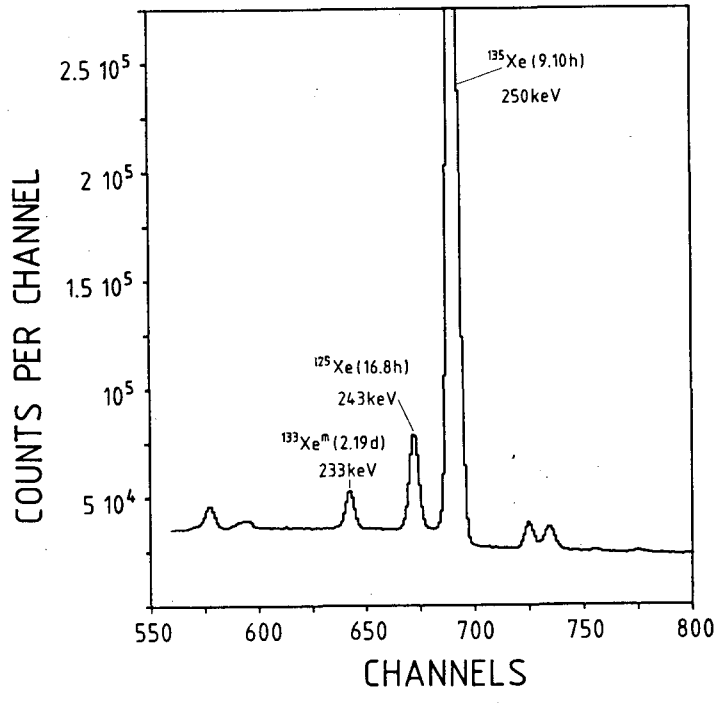

Fig. 1 A section of the accumulated data with activity lines from the reactions $^{132}Xe(n,\gamma)\,^{133}Xe^{m}$, $^{124}Xe(n,\gamma)\,^{125}Xe$ (16.8 h), $^{134}Xe(n,\gamma)\,^{135}Xe$ (9.10 h).

selectivity of the activation technique was used to determine these capture cross sections with samples of natural composition.

The measurements were carried out by fast cyclic activation. This technique is an extension of the conventional activation method (1) which can be applied conveniently only to nuclei with half lives ≥ 0.5 h. The present setup, however, allows for the simultaneous measurement of activities with half lives ≥ 10 s. The samples consisted of a mixture of natural Kr and Xe gas contained into stainless steel spheres [20 mm dia, 0.5mm wall thickness]. The half lives of the activities to be counted ranged from 13 s to 36.4 d. In the runs it was posible to measure 5 isotopic Kr cross sections and 11 isotopic Xe cross sections. The following reactions are especially interesting:

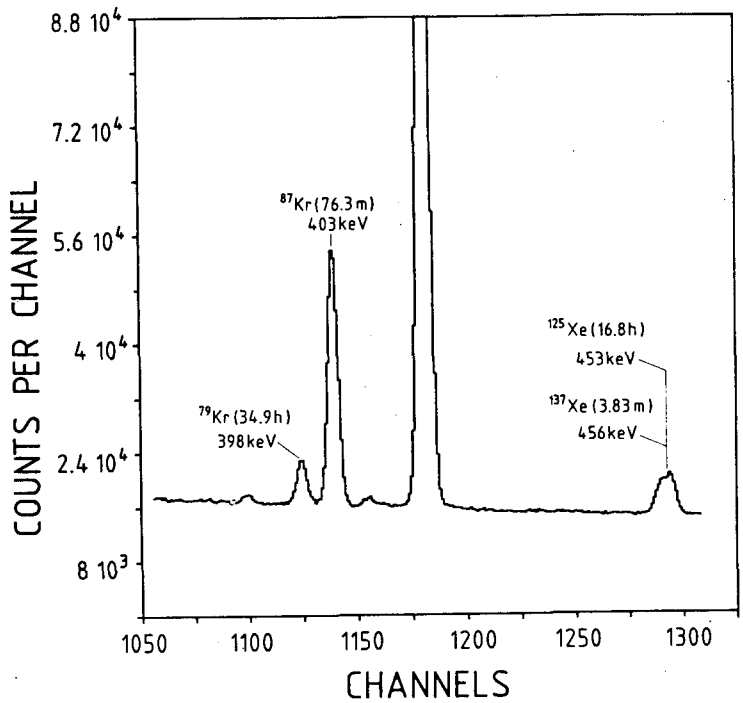

Fig. 2 A section of the accumulated data with lines corresponding to the reactions $^{78}Kr(n,\gamma)\,^{79}Kr$ (34.9 h), $^{86}Kr(n,\gamma)\,^{87}Kr$ (76.3 m) $^{124}Xe\,(n,\gamma)\,^{125}Xe$ (16.8 h), $^{136}Xe\,(n,\gamma)\,^{137}Xe$ (3.83 m).

(1) The reactions $^{128}Xe(n,\gamma)\,^{129}Xe^{m}$ (8.89d) and $^{130}Xe(n,\gamma)\,^{131}Xe$ (11.9d) will be used for a better assessment of the corresponding total capture cross sections of these two s-only isotopes.

(2) The very small $^{136}Xe(n,\gamma)\,^{137}Xe$ (3.83 m) cross section is an important input quantity for the analysis of the isotopic Xe anomalies (2).

The figures 1 and 2 show two parts of an accumulated spectrum with the characteristic γ ray lines of the activated nuclei. The 456 keV line to determine the ^{136}Xe capture cross section overlaps with a line at 453 keV from the ^{125}Xe (16.8 h) decay (Fig. 2). But a separation of the intensities is obtained using another ^{125}Xe line at 243 keV (Fig. 1) and the well known intensity ratio of the 453 and 243 keV lines.

(1) H. Beer, F. Käppeler, Phys. Rev. **C21**, 534 (1980)
(2) D.D. Clayton, Ap J **340**, 613 (1989)

2. ^{88}Sr AND ^{89}Y: THE s-PROCESS AT MAGIC NEUTRON NUMBER N=50

F. Käppeler, W. Zhao*, H. Beer, U. Ratzel

The neutron capture cross sections of ^{88}Sr and ^{89}Y were measured in a quasi-stellar neutron spectrum for kT = 25 keV via the activation method. Relevant systematic uncertainties were determined experimentally by repeated activations under different conditions and with different samples. Gold was used as a cross section standard. The resulting stellar cross sections for kT = 30 keV are 6.13 ± 0.18 mb for ^{88}Sr and 19.0 ± 0.6 mb for ^{89}Y. The partial cross section $^{86}Sr(n,\gamma)^{87m}Sr$ was measured to 48.1 ± 1.2 mb. Compared to previous data, the associated uncertainties are reduced by factors of 3 and 5, respectively. The implications for s-process nucleosynthesis around magic neutron number N = 50 are discussed in the light of new information on neutron density and temperature.

(1) The Astrophysical Journal (in print)

* On leave from Institute of Atomic Energy, Academica Sinica, Beijing, People's Republic of China

3. THE STELLAR NEUTRON CAPTURE CROSS SECTIONS OF ^{94}Zr AND ^{96}Zr

K.A. Toukan*, F. Käppeler

The neutron capture cross sections of $^{94,96}Zr$ have been determined relative to that of gold by means of the activation method. The samples were irradiated in a quasi-stellar neutron spectrum for kT = 25 keV using the $^{7}Li(p,n)^{7}Be$ reaction near threshold. Variation of the experimental conditions in different activations and the use of different samples allowed to reliably determine corrections and to evaluate systematic uncertainties. The resulting stellar cross sections can be given with uncertainties around 4%, considerably lower than previous data. The new data allowed for the first time to deduce the s-process neutron density from the branching at ^{95}Zr.

(1) The Astrophysical Journal **348**, 357 (1990)

* On leave from University of Jordan, Amman, Jordan

4. THE s-PROCESS BRANCHING AT ^{185}W AND ^{186}Re.

F. Käppeler, Z.Y. Bao*, G. Reffo, S.N. Wang*

Nucleosynthesis in the mass region between tungsten and osmium has received considerable attention, mostly due to the possible use of ^{187}Re as a chronometer for the r-process. Figure 1 illustrates the s-process flow through the W-Re-Os isotopes and the corresponding contributions from the r-process beta decay chains. Obviously, ^{186}Os and ^{187}Os are shielded against the r-process by their isobars, and hence are produced as pure s-process isotopes. However, ^{187}Os has received an additional abundance contribution from the decay of ^{187}Re, which is predominantly produced in the r-process. The s-process part of the ^{187}Os abundance can be reliably determined as the σN values of ^{186}Os and ^{187}Os are known to be equal according to the 'local approximation'. The excess in the ^{187}Os abundance can then be ascribed to the decay of ^{187}Re, which therefore was long considered as a chronometer for the r-process (1, 2, 3).

The quantitative interpretation of the chronometer pair ^{187}Re-^{187}Os is, however, complicated by the influence of stellar temperature and pressure on the decay of ^{187}Re (4), but also by problems concerning the stellar neutron capture rate of ^{187}Os (5), and the chemical evolution of galactic material (6, 7). Apart from their importance for cosmochronometry, the isotopes ^{186,187}Os are of interest as normalization points for the s-process branchings at ^{185}W and ^{186}Re, which are indicated in figure 1. These branchings define the small s-process contribution to

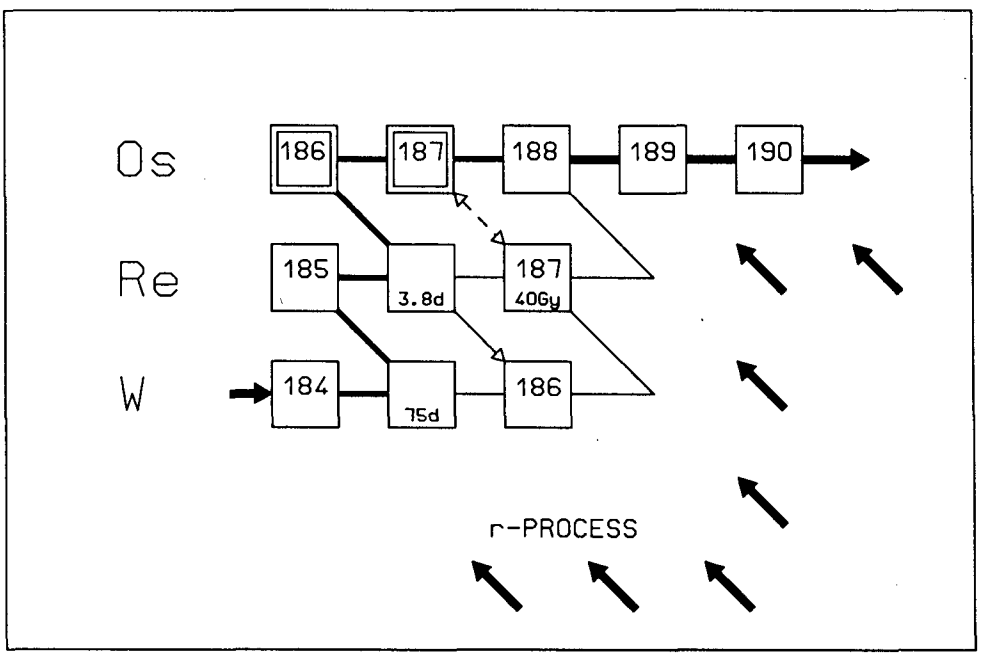

Fig. 1 The s-process flow through the W-Re-Os isotopes.

the ^{187}Re abundance, but are mainly useful for estimating the mean neutron density during the s-process. It is important in this respect that the beta decay rates of the branch point isotopes ^{185}W and ^{186}Re are almost unaffected at typical s-process temperatures (4). The main uncertainty in previous analyses of these branchings (7, 8, 9) resulted from the cross sections of the branch point isotopes. These data were obtained by statistical model calculations with a parametrization for a wide mass range (10, 11), and are estimated to be uncertain by a factor of two. Moreover, the available experimental data for the stable Re isotopes showed uncertainties of typically 10 to 20%, but differed by up two 100%. A new and accurate measurement of the stellar cross sections for ^{185}Re and ^{187}Re has therefore been initiated in order to complete a reliable set of cross section data for the stable isotopes in the mass range of interest. In turn, these data could be used to establish and to check a consistent local parameter systematics for improved statistical model calculations for the relevant branch point nuclei ^{185}W and ^{186}Re.

The measurements were carried out at the Karlsruhe Van de Graaff accelerator via the activation technique, using the quasi stellar neutron spectrum at kT = 25 keV (12, 13). After irradiation of a sample sandwich consisting of metallic rhenium and gold foils, the induced activities were counted with a HPGe detector in a low background environment. Figure 2 shows the gamma-ray spectrum measured after irradiation of a 14.7 mg Re sample for 5.4 h. The background ist mostly due to beta decay electrons and appears rather high,

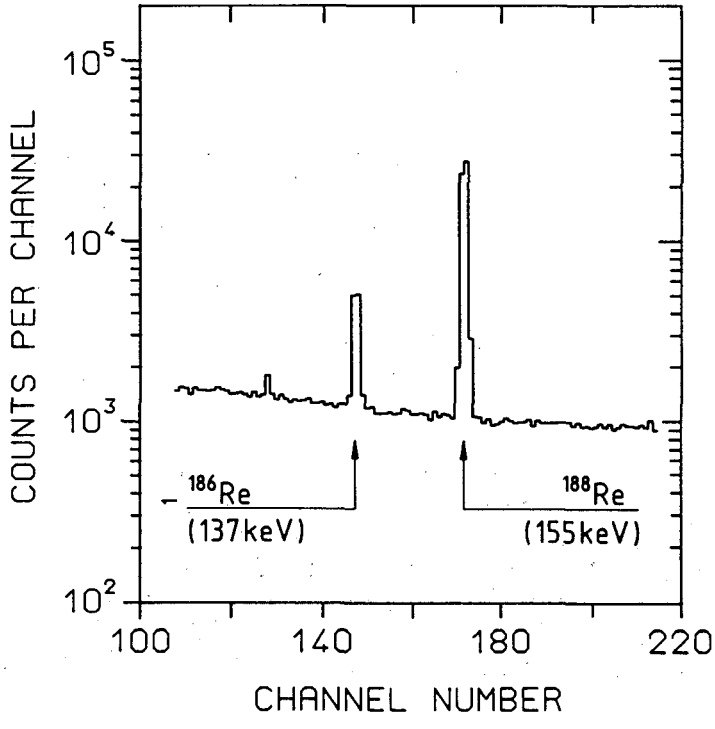

Fig. 2 Gamma-ray spectrum of a 14.7 mg Re sample measured after activation.

because the relative intensities of both gamma-ray transitions are relatively weak. Nevertheless, the signal to background ratios are high enough to allow for counting statistics well below 1%. This holds the more for the gold activity, which was determined via the 411.8 keV transition. The various uncertainties were carefully evaluated by repeated activations with systematically modified experiment parameters. The resulting cross sections are $<\sigma v> / v_T = 1689 \pm 65$ mb and 1269 ± 62 mb for ^{185}Re and ^{187}Re, respectively. The basic idea for refining statistical model calculations of neutron capture cross sections is to evaluate a local systematics of the relevant model parameters for the neighboring stable isotopes, including as much experimental information as possible. The concept of the adopted technique has been described previously (e.g. 17, 18). For the present cases the level density parameter a for the compound systems ^{186,188}Re was deduced from the spacing of s-wave neutron resonances, and at low excitation energies from the respective level schemes. Spin and parity distributions were also carefully considered, and the so obtained parametrization has been tested by comparison of the calculated average radiative widths at the neutron binding energy with experimental values. An uncertainty of 20% was estimated for the calculated cross sections by considering the uncertainties in the involved parameters.

With the new information on the relevant cross sections, the s-process branchings at ^{185}W and ^{188}Re have been reanalyzed in terms of the classical approach. The deduced s-process neutron density of

$$n_n = (4.1 \; {}^{+1.2}_{-1.1}) \cdot 10^8 \, cm^{-3}$$

is in good agreement with other branchings in the mass range $A < 100$ (14).

(1) E.M.D. Symbalisty, D.N. Schramm, Rep. Prog. Phys. **44** (1981) 293
(2) J.C. Browne, B.L. Berman, Phys. Rev. **C23** (1981) 1434
(3) R.R. Winters, R.L. Macklin, Phys. Rev. **C25** (1982) 208
(4) K. Takahashi, K. Yokoi, Atomic Data and Nuclear Data Tables **36** (1987) 375
(5) R.R. Winters, R.F. Carlton, J.A. Harvey, N.W. Hill, Phys. Rev. **C34** (1986) 840
(6) K. Yokoi, K. Takahashi, M. Arnould, Astron. Astrophys. **117**, (1983) 65
(7) M. Arnould, K. Takahashi, K. Yokoi, Astron. Astrophys. **137** (1984) 51
(8) H. Beer, G. Walter, R.L. Macklin, P.J. Patchett, Phys. Rev. **C30** (1984) 464
(9) H. Beer, R.L. Macklin, Ap. J. **331** (1988) 1047
(10) J.A. Holmes, S.E. Woosley, W.A. Fowler, B.A. Zimmerman, Atomic Data and Nuclear Data Tables 18 (1976) 305
(11) M .J. Harris, Astrophys. Space Sci. **77** (1981) 357
(12) H. Beer, F. Käppeler, Phys. Rev. **C21** (1980) 534
(13) W. Ratynski, F. Käppeler, Phys. Rev. **C37** (1988) 595
(14) F. Käppeler, R. Gallino, M. Busso, G. Picchio, C.M. Raiteri, Ap. J. (1990) in press

* On leave from the Institute of Atomic Energy, Beijing, People's Republic of China

5. A NEW APPROACH FOR PRECISE MEASUREMENTS OF keV NEUTRON CAPTURE CROSS SECTIONS : THE EXAMPLES OF NIOBIUM, RHODIUM AND TANTALUM

K. Wisshak, F. Voß, F. Käppeler, G. Reffo* (1)

A new experimental method has been implemented for high precision measurements of neutron capture cross sections in the energy range from 5 to 200 keV. Neutrons are produced via the $^{7}Li(p,n)^{7}Be$ reaction using a pulsed 3 MV Van de Graaff accelerator. The neutron energy is determined by the time of flight technique using a flightpath of less than 1 m. Capture events are detected with the Karlsruhe 4π Barium Fluoride Detector. This detector combines a gamma ray energy resolution of 14% at 662 keV and 7% at 2.5 MeV and a time resolution of

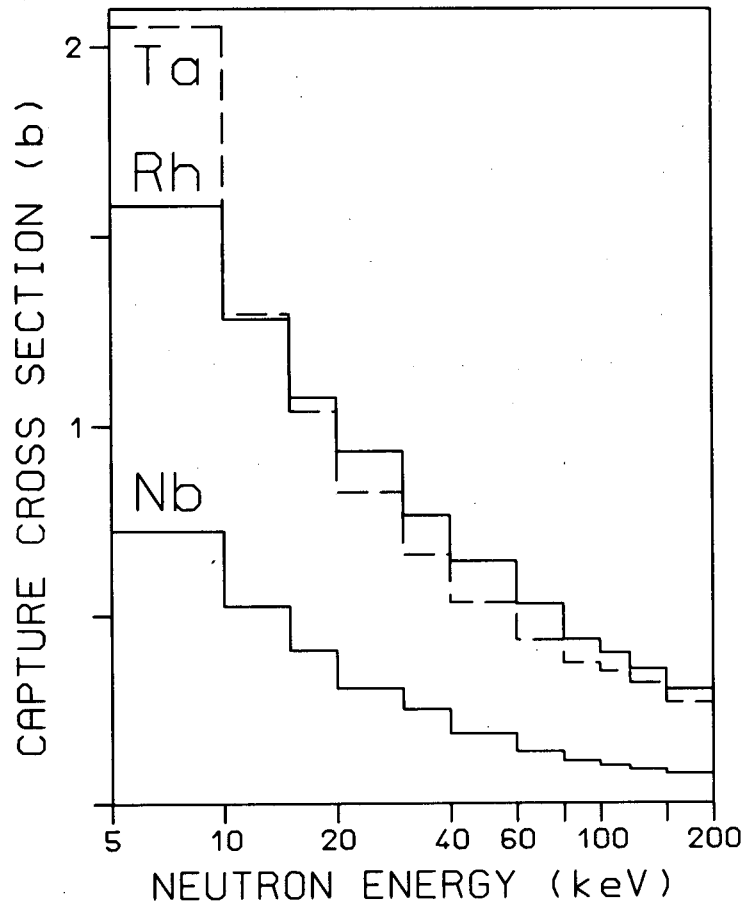

Fig. 1 The neutron capture cross sections of ^{93}Nb, ^{103}Rh and ^{181}Ta in the energy range fom 5 to 200 keV.

500 ps with a peak efficiency of 90% at 1 MeV. Capture events are registered with ~95% probability above a gamma ray threshold of 2.5 MeV.

The combination of short flight path, 10 cm inner radius of the detector and low capture cross section of BaF_2 allows to discriminate background due to capture of sample scattered neutrons in the scintillator material by time of flight leaving part of the neutron energy range completely undisturbed. The high efficency and good energy resolution for capture gamma-rays allows to reduce this background further by selecting appropriate energy channels for data evaluation.

The first test measurements were made on ^{93}Nb, ^{103}Rh and ^{181}Ta; neutron capture cross sections were determined in the energy range from 3 to 200 keV relative to a gold standard. The cross section ratio could be determined with an overall systematic uncertainty of 0.7 - 0.8% and a statistical uncertainty of less than 1% in the energy range from 20 to 100 keV if the data are combined in 20 keV wide bins. The necessary sample masses were of the order of one gram. The accuracy of the experimental method will be further increased and simultaneously the required sample mass will be reduced by several improvements already implemented or under development.

In Fig. 1 values for the absolute cross sections are plotted that are obtained by multiplying the experimental ratio with the gold cross section known from literature. The uncertainty of these values is dominated by the 1.5% uncertainty in the absolute normalization by the gold cross section.

(1) Report KfK 4674, Kernforschungszentrum Karlsruhe
(submitted for publication in Phys. Rev. C)

* ENEA, Bologna, Italy

KERNFORSCHUNGSZENTRUM KARLSRUHE
INSTITUT FÜR MATERIAL- UND FESTKÖRPERFORSCHUNG II

1. Investigation of Element Activation by Sequential (x,n) Reactions

S. Cierjacks, Y. Hino[1]

The investigations of the effects of so-called "sequential (x,n) reactions" on fusion materials activation have been continued. Sequential (x,n) reactions are processes in which charged particles x , produced in a primary step A(n,x)B, react in a subsequent step by A(x,n)C with the nucleus A producing the residual nucleus C. Since the nucleus C is not produced by any of the primary neutron-induced reactions, this gives rise to additional radioactivities if either this nucleus itself or any subsequent built-up product of C is unstable. Such contributions to the induced radioactivity have been neglected in all investigations heretofore. While our early work was restricted to some sequential (x,n) reactions on ^{56}Fe, these studies have been extended to more nuclides, reactions, and global activation calculations, the latter of which showing the importance of such processes on the integral element activation and/or the related radiological properties such as surface γ-dose rates, decay heats, and biological hazards [1-3]. A summary of elements and sequential (x,n) reactions investigated up to now is given in Table I. This table lists the important radionuclides produced by sequential (p,n), (d,n) and (α,n) reactions on Na, Mg, V, Cr and Fe. The total induced inventories and the activities in the first wall of a DEMO fusion reactor at shut-down are given in columns 4 and 5. The numerical values in these columns are total quantities which might have been produced by more than one sequential reaction (see column 6). An extreme example of the

Table I. Important radioisotopes produced in element activation by sequential (x,n) reactions.

Element	Radio-Isotope	Halflife (y)	Induced Inventory (at./kg)	Activity at Shutdown (Bq/kg)	Important Sequential Reactions
Na	^{26}Al	7.2×10^{5}	5.2×10^{18}	1.6×10^{5}	^{23}Na(α,n)^{26}Al
Mg	^{26}Al	7.2×10^{5}	1.2×10^{18}	3.7×10^{4}	^{26}Mg(p,n)^{26}Al ^{25}Mg(d,n)^{26}Al
V	^{53}Mn ^{54}Mn	3.7×10^{6} 8.5×10^{-1}	1.8×10^{15} 8.3×10^{16}	1.1×10^{1} 2.1×10^{9}	^{50}V(α,n)^{53}Mn ^{51}V(α,n)^{54}Mn
Cr	^{53}Mn	3.7×10^{6}	1.5×10^{18}	8.9×10^{3}	^{53}Cr(p,n)^{53}Mn ^{52}Cr(d,n)^{53}Mn ^{50}Cr(α,n)^{53}Mn
	^{55}Fe	2.7×10^{0}	2.3×10^{17}	1.9×10^{9}	^{52}Cr(α,n)^{55}Fe
Fe	^{56}Co ^{57}Co ^{59}Ni	2.2×10^{-1} 7.4×10^{-1} 7.5×10^{4}	5.6×10^{17} 1.9×10^{17} 2.7×10^{17}	6.3×10^{10} 5.6×10^{9} 7.9×10^{4}	^{56}Fe(p,n)^{56}Co ^{56}Fe(d,n)^{57}Co ^{56}Fe(α,n)^{59}Ni

KfK calculations performed up to now is the production of ^{26}Al through the sequential reaction $^{23}Na(n,\alpha)^{20}F + ^{23}Na(n,z\alpha) \rightarrow ^{23}Na(\alpha,n)^{26}Al$ (z stands for any particle other than α). This is illustrated in Fig. 1 which shows the integral surface γ-dose rate of sodium versus time after irradiation. For eliminating the effects of the sequential (α,n) reaction, the dose rates were calculated twice: Once with and once without inclusion of this reaction, while leaving all other calculational conditions unchanged. It can be seen that the contribution of the sequential the $^{23}Na(\alpha,n)^{26}Al$ reaction is most pronounced in the time range beyond ~100 y, where the top curve is governed by the ^{26}Al-activity ($T_{1/2} = 7.2 \times 10^5$ y). Inclusion of the sequential (α,n) reaction alters the dose rates by 9 orders of magnitude; it even places the long-time dose rates significantly above the "hands-on" level of 2.5×10^{-5} Sv/h. Important effects between 1 and 4 orders of magnitude have also been found for some of the integral radiological quantities of Mg, V and Cr in different regions of cooling times between 1 and 10^6 years [1,2].

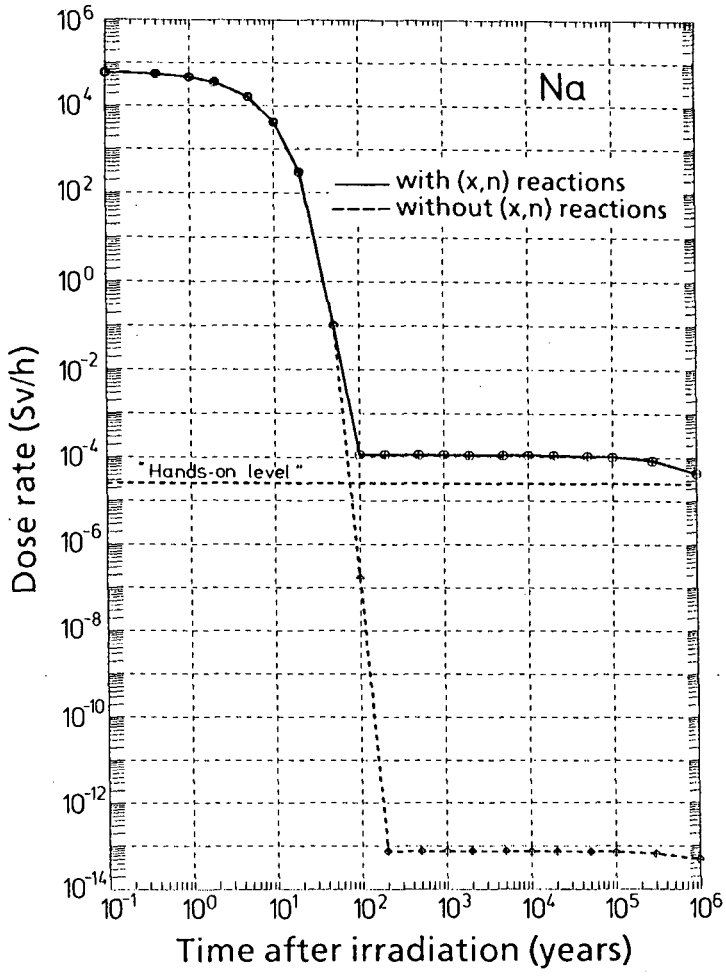

Fig. 1 Calculated dose rate versus cooling time for Na. The results refer to neutron irradiation in the first wall of a DEMO fusion reactor. A 1st wall neutron load of 12.5 MW a m^{-2} was assumed. The difference between the two curves is a measure of the contribution of the ^{26}Al-activity ($T_{1/2} = 7.2 \times 10^5$ y) produced by the sequential $^{23}Na(\alpha,n)^{26}Al$ reaction.

2. Production of Nuclear Data Libraries for the Treatment of Sequential (x,n) Reactions in Global Activation Calculations

S. Cierjacks, Y. Hino[1], K. Anderko

Due to the observed importance of sequential (x,n) reactions for fusion materials activation (see Topic 1.), work has been started to produce new libraries required for the inclusion of these reactions in kinematically complete activation calculations [4]. In general, the inclusion of sequential (x,n) reactions requires three types of new libraries, not yet contained in any of the currently existing activation files: (1) Double-differential neutron-induced charged-particle emission cross sections, (2) energy-dependent charged-particle reaction cross sections, and (3) energy-dependent stopping powers for all kinds of secondary charged particles and potential alloying and unavoidable tramp impurity elements. In a first step, it is intended to produce the libraries for a complete treatment of (p,n), (d,n), (α,n) and (t,n) sequential reactions in all isotopes with $A \leq 100$ and half-lifes ≥ 1 day. These reactions and isotopes are expected to give the most important contributions to the integral radiological quantities. Preparations are being made to obtain the data from the follwing sources: (1) A factorization of the double-differential cross sections by $\sigma_{n,x}(E_n,E_x) = \sigma_{n,x}(E_n) \times f(E_x)$ allows the excitation functions $\sigma_{n,x}(E_n)$ to be taken from the European Activation File (EAF), and the normalized charged-particle energy-distribution functions $f(E_x)$ from suitable cross section systematics. For the energy-dependent charged-particle reaction cross sections experimental results are to a certain extent available from the Obninsk Data Center and Münzel's [5] compilations. For the unknown charged particle cross sections the semi-empirical method proposed by Keller et al. [6] can be employed. Charged-particle stopping powers are readily available from Ziegler's work [7]. For computer-aided tabulations a suitable KfK code is available.

3. Nuclear Data Needs for Low-Activation Materials Development

S. Cierjacks, K. Anderko

So-called "low-activation" materials (LAMs) are presently considered as an important means for improving the safety and environmental characteristcs of future DT fusion reactors. Present programs on low-activation materials development depend strongly on reliable activity estimates for a wide range of technologically important elements including unavoidable tramp impurity elements. The general nuclear data needs for this field have been surveyed [4,8]. Primarily, energy-dependent neutron activation cross sections and nuclear decay data for a large number of stable and radioactive nuclides are required. In addition, other nuclear and atomic data such as Bremsstrahlung data (for the estimate of dose rates and decay heats), double-differential neutron cross sections, energy-dependent charge-particle reaction cross sections, and charged-particle stopping powers (for the treatment of sequential (x,n) reactions) or CEDE factors (for the prediction of biological hazards) are

necessary. The present status of existing data libraries has been reviewed and critically examined; lacking or unsufficiently known data are identified. The most critical data which immediately need major effort are summarized.

4. Proposal for a Novel High-Intensity 14-MeV Cutoff Neutron Source for Fusion Materials Testing

S. Cierjacks, Y. Hino[1], M. Drosg[2], K. Ehrlich

In continuation of our studies on neutron production aspects of the $^1H(t,n)^3He$ source reaction [9,10], a conceptual design for a high-intensity 14-MeV cutoff neutron source based on this reaction has been worked out [11]. Utilizing the $^1H(t,n)^3He$ reaction and bombarding thick hydrogen-rich targets with intense beams of 21-MeV tritons provides a powerful

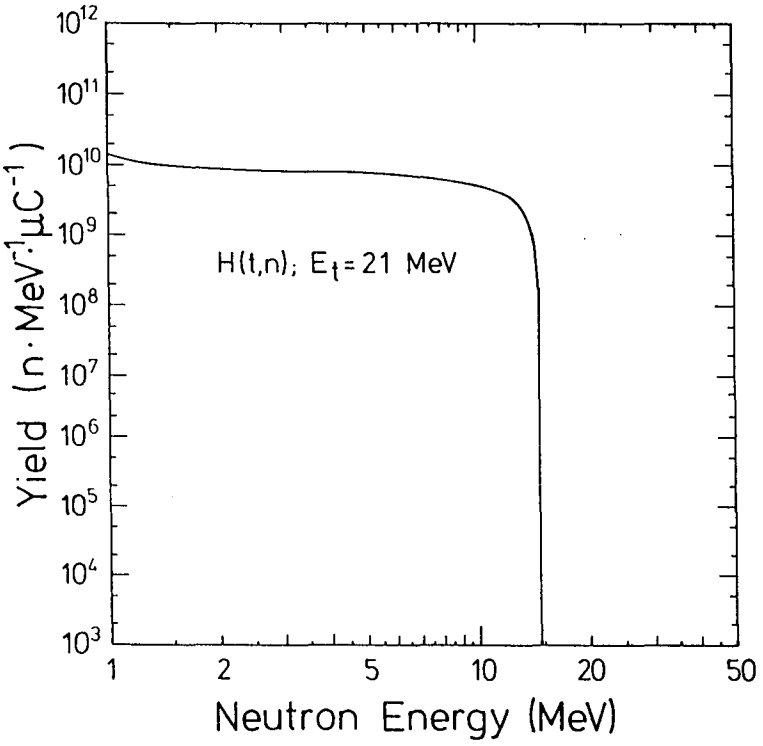

Fig. 2. "Gross" neutron spectrum produced by the $^1H(t,n)^3He$ reaction with 21 MeV tritons [11]. The spectrum shows angle-integrated yields over the whole range of emission angles from 0-67° scaled by the solid angle.

"white" neutron source. To meet near-term needs for fusion materials testing, a reference design is proposed that involves multiple linear-accelerator modules for producing two 250-mA triton beams to bombard two thick water jet targets. The targets are arranged in facing geometry and irradiate the same test volume. When a relative orientation angle of 120° is used, average neutron fluxes of $\geq 1 \times 10^{19}$ n m^{-2} s^{-1} can be achieved in a volume 160

cm^3. Fluxes of $\geq 1 \times 10^{18}$ n m^{-2} $s^{-1}$are achievable in a volume of 4.2 dm^3. The outstanding feature of the proposed source is a high spectral intensity over the range from 1 to 14 MeV and a sharp cutoff energy of 14.6 MeV (see Fig. 2). In addition to the special $^1H(t,n)^3He$-source study, some surveys on the present status and the future potential of neutron sources for neutron physics, nuclear data measurements and fusion technology have been coordinated and performed [12-14].

---

1 On leave from Electrotechnical Laboratory, 1-1-4 Umezono, Ibaraki, Japan
2 Institut für Experimentalphysik, University of Vienna

References

[1] S. Cierjacks and Y. Hino; The influence of sequential (x,n) reactions on total element activities; J. Nucl. Mater. 170, 134 (1990).

[2] S. Cierjacks and Y. Hino; The Role of sequential (x,n) reactions on element activation of fusion reactor materials and related nuclear data needs; Proc. NEANDC Specialists Meeting on Neutron Activation Cross Sections for Fission and Fusion Energy, Argonne, September, 13-15, 1989, eds. M. Wagner, H. Vonach, NEA Paris, p. 19, 1990.

[3] S. Cierjacks and Y. Hino; Sequential (x,n) reactions: An important reaction mechanism for element activation of fusion reactor materials; Session 7-D3, 4th Intern. Conf. on Fusion Reactor Materials, Kyoto, Japan, December 4-8, 1989.

[4] S. Cierjacks; Nuclear data needs for low-activation fusion materials development; Fusion Engrg. Des. 13, in press.

[5] K.A. Keller, J. Lange, H. Münzel and G. Pfennig; Excitation functions for charged-particle induced nuclear reactions; in Landolt-Börnstein Vol. 5/1, Part b, ed. H. Schopper, Springer Verlag, Berlin, 1973.

[6] K.A. Keller, J. Lange, and H. Münzel; Estimation of unknown excitation functions and thick target yields for p, d, ^3He and α reactions; in Landolt-Börnstein Vol. 5/1, Part c, ed. H. Schopper, Springer Verlag, Berlin, 1973.

[7] J.F. Ziegler, Handbook of Stopping Cross Sections for Energetic Ions in All Elements, ed. J. F. Ziegler, Pergamon Press, 1980.

[8] S. Cierjacks; Low-activation fusion materials development and related nuclear data needs; IAEA Advisory Group Meeting on the Status and Requirements of Nuclear Data for Radiation Damage and Related Safety Aspects, Vienna September 19-22, 1989, IAEA-TECDOC, in press.

[9] S. Cierjacks; High-energy neutron production by the $^{1}H(t,n)^{3}He$ source reaction; Proc. Internat. Fusion Materials Irradiation Facility (IFMIF) Workshop for the International Energy Agency, San Diego, February 14-17, 1989, p.329, ed. R. Verbeek, Commission of the European Communities, Brussels, Belgium, 1990.

[10] S. Cierjacks: High-intensity 14-MeV cutoff neutron production by the $^{1}H(t,n)^{3}He$ source reaction: J. Fusion Energy 8, 193 (1990).

[11] S. Cierjacks, Y. Hino, and M. Drosg; Proposal for a high-intensity 14-MeV cutoff neutron source based on the $^{1}H(t,n)^{3}He$ source reaction; Nucl. Sci. Eng. 106, in press.

[12] S. Cierjacks, K. Ehrlich, E.T. Cheng, H. Conrads and H. Ullmaier; High-intensity fast neutron sources and neutron fields for fusion technology and fusion materials research; Nucl. Sci. Eng. 106, in press.

[13] S. Cierjacks, Guest Editor; Special Issues of NS&E on "Neutron Sources for Fusion Technology and Fusion Materials Research"; to be published in the October and November 1990 Volumes of NS&E.

[14] Summary Report of the NEANDC Working Group on Intense Neutron Sources for Neutron Physics and Nuclear Data Measurements, ed. S. Cierjacks, NEANDC Report, NEANDC-274-A, December 1989.

KERNFORSCHUNGSZENTRUM KARLSRUHE

INSTITUT FÜR NEUTRONENPHYSIK UND REAKTORTECHNIK

Nuclear Data Evaluation

1. Evaluation of Neutron Resonance Cross Sections for Stable Iron Isotopes

F.H. Fröhner

A new evaluation of the resonance cross sections of the natural iron isotopes ^{54}Fe, ^{56}Fe, ^{57}Fe and ^{58}Fe is in progress for the second version of the Joint Evaluated File, JEF-2, and for the corresponding update of the European Fusion File, EFF-2. The following table shows the main characteristics.

Table 1 - Evaluation of Fe cross sections for EFF-2

Isotope	Abundance (%)	Energy Range (keV)	Number of Levels	Resonance Formalism
^{54}Fe	5.8	0 - 500	164	1-channel Reich-Moore
^{56}Fe	91.7	0 - 862	286	1-channel Reich-Moore
^{57}Fe	2.2	0 - 200	121	2-channel Reich-Moore
^{58}Fe	0.3	0 - 370	93	1-channel Reich-Moore

The evaluation of resonance parameters for consistent pointwise calculation of total, capture, elastic and (for ^{57}Fe) inelastic scattering cross sections is completed. The starting point was EFF-1 which, for iron resonance cross sections, is basically the KfK evaluation KEDAK-4 [1, 2]. This was updated with experimental results that have become available in recent years, mainly from Geel, ORNL, Harwell and KfK [3, 4].

The resonance parameter evaluation is completed, covariance files remain to be established. The Reich-Moore formalismus was adopted in order to guarantee a good description of the pronounced s-wave resonance minima in the total cross sections ("windows") that are important for shielding applications. As inelastic scattering is energetically forbidden in the range of the evaluation the 1-channel version of the formalism suffices with the exception of ^{57}Fe which has one open inelastic s-wave channel above 14 keV. Over the wide energy ranges considered the energy dependence of potential scattering caused by distant levels must be taken into account. Since the ENDF-6 format adopted for JEF-2 and EFF-2 does not accomodate the usual statistical description of their influence a new prescription was derived from R-matrix theory (see following section).

2. Evaluation Methods: ENDF-Compatible Distant-Level Description

F.H. Fröhner

The influence of distant levels, i. e. of unknown levels below and above the region of explicitly known resolved resonance parameters, can be calculated statistically. In the Reich-Moore formalism their contribution to the diagonal elements of the reduced R-matrix is [5] :

$$R^0 = R^\infty + 2s\left(\text{ar tanh } x + i\,\frac{\bar{\Gamma}_\gamma/I}{1-x^2}\right) \qquad \text{with} \qquad x \equiv \frac{E-\bar{E}}{I/2}\,,$$

where $\bar{E}$ and I are midpoint and length of the region of known resolved resonances. Three level-statistical parameters are involved: the distant-level parameter R^∞ (related to the effective nuclear radius R′ and the channel radius a by $R' = a(1-R^\infty)$), the pole strength s (related to the familiar strength function S by $S = 2k_1 a\, s$, k_1 being the entrance channel wave number for 1 eV of incident energy), and the average radiation width $\bar{\Gamma}_\gamma$. This description of the influence of distant levels is not possible under present ENDF-6 rules. The main features can, however, be reproduced with two fictitious resonances, one below and one above the range of known resonances,

$\bar{E} - I/2 \ldots \bar{E} + I/2$. Expanding both the level-statistical expression for R^0 and the resonance pair contribution around $E = \bar{E}$, and equating the coefficients of the leading terms, one finds

$$E_- = \bar{E} - \sqrt{3}\,\frac{I}{2}\,, \qquad \Gamma_{n-} = 3IP(|E_-|)s\,, \qquad \Gamma_{\gamma-} = \bar{\Gamma}_\gamma\,,$$

$$E_+ = \bar{E} + \sqrt{3}\,\frac{I}{2}\,, \qquad \Gamma_{n+} = 3IP(E_+)s\,, \qquad \Gamma_{\gamma+} = \bar{\Gamma}_\gamma\,,$$

for the parameters of the resonance pair, where P is the usual centrifugal-barrier penetrability.

The Figure shows the relevant functions of x in the real and imaginary part of R^0 for the level-statistical expression (solid curves) and for the resonance pair approximation (dashed curves). The approximation was tried in the evaluation of resonance cross sections for Fe isotopes described above and yielded, together with one bound level per s-wave channel, a good description of potential scattering from thermal energies all the way up to the end of the resolved resonance range.

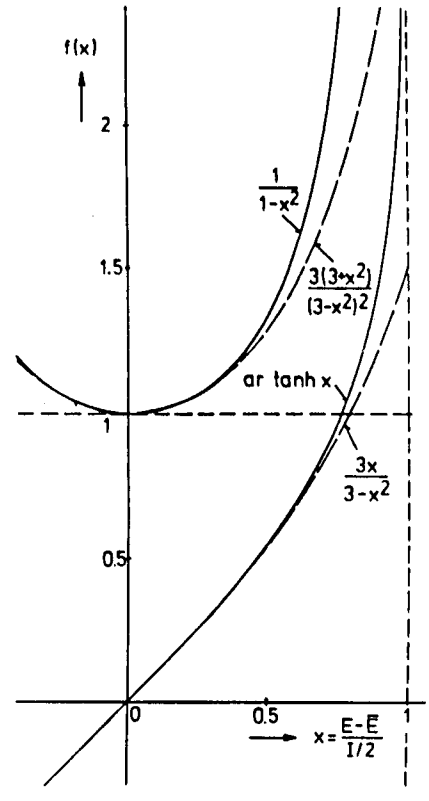

References

[1] F.H. Fröhner, in "Neutron Data for Structural Materials", Conf. Proc. Geel 1977, Pergamon Press (1978) p. 138

[2] B. Goel, B. Krieg, Report KfK 3838 (1984)

[3] S.F. Mughabghab et al., Neutron Cross Sections, Acad. Press (1981) Vol. 1, Part A

[4] CINDA89, IAEA, Vienna (1989)

[5] F.H. Fröhner, Proc. Conf. Nucl. Data Eval. Meth. and Proced., BNL 1980, BNL-NCS-51363 (1981) vol. 1 p. 375

INSTITUT FÜR CHEMIE (1): NUKLEARCHEMIE FORSCHUNGSZENTRUM JÜLICH

1. Neutron Data

1.1 Systematics of Excitation Functions of (n,t) Reactions

S.M. Qaim, R. Wölfle, G. Stöcklin

In continuation of our fundamental studies on nuclear reactions involving complex particle emission the excitation functions of (n,t) reactions on ^{139}La and ^{209}Bi were measured in the energy range of 15 to 20 MeV (in collaboration with H. Liskien and R. Widera, CBNM Geel). Information exists now on excitation functions of (n,t) reactions on ^{6}Li, ^{7}Li, ^{9}Be, ^{10}B, ^{14}N, ^{27}Al, ^{51}V, ^{59}Co, ^{93}Nb, ^{115}In, ^{181}Ta and ^{209}Bi. A systematic analysis of the available excitation functions has now been completed. The cross sections of (n,t) reactions on the light mass nuclei (^{6}Li to ^{14}N) are high; in some cases (e.g. ^{14}N) the excitation function shows fluctuations due to nuclear structure effects. In the medium mass region (^{27}Al to ^{93}Nb), at a given incident neutron energy the (n,t) cross section decreases with the increasing mass of the target nucleus. For heavier mass target nuclei (^{93}Nb to ^{209}Bi) the (n,t) cross section at $E_n \approx 20$ MeV remains practically constant (for details cf. [1]).

1.2 Study of (n,^{7}Be) Reactions

B. Scholten, S.M. Qaim, G. Stöcklin

In continuation of our radiochemical studies on ^{7}Be emission (cf. last Progress Report) several other elements were irradiated with 53 MeV d(Be) breakup neutrons. Chemical processing of the irradiated material and γ-ray spectroscopic analysis of the separated samples are in progress. Investigations are underway so far on ^{28}Si, ^{51}V, ^{55}Mn, ^{59}Co, ^{75}As, ^{93}Nb, ^{197}Au and ^{209}Bi. The (n,^{7}Be) cross section appears to be very low (nb-μb region).

1.3 Isomeric Cross-Section Ratios

N.I. Molla, M. Ibn Majah, R. Wölfle, S.M. Qaim

Continuing our studies on isomeric cross-section ratios [2] we investigated the $^{90}Zr(n,p)^{90m,g}Y$ and $^{91}Zr(n,p)^{91m,g}Y$ processes in the energy range of 6.5 to 10.6 MeV. Statistical model calculations taking into account precompound effects were performed (in collaboration with B. Strohmaier, IRK Vienna). The results for the $^{91}Zr(n,p)^{91m,g}Y$ process are shown in Fig. 1. There appears to be good agreement between experiment and theory up to 9 MeV; at higher energies the calculated values are consistently higher. The amount of preequilibrium proton emission is thus described correctly as a function of incident energy; its spin distribution, however, appears to be approximated poorly by the formulation used (for details cf. [3]).

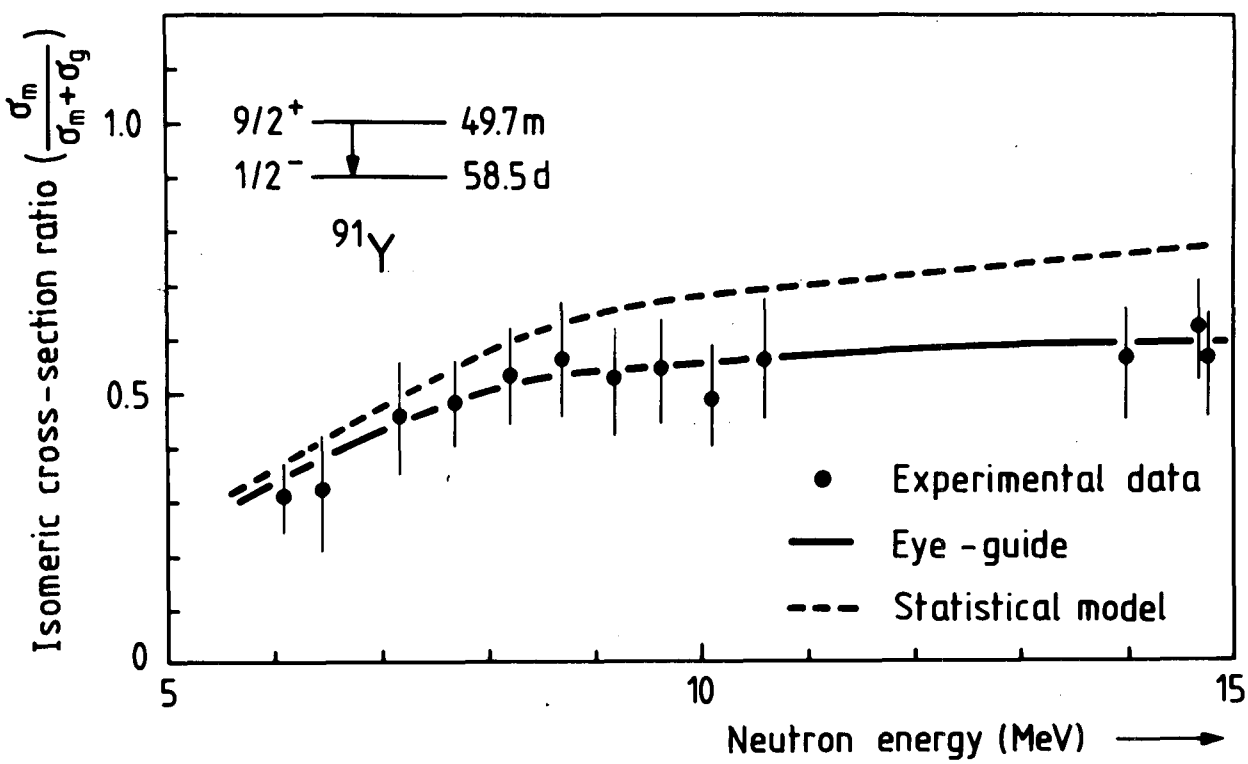

Fig. 1 Isomeric cross-section ratio for the isomeric pair $^{91m,g}Y$ [formed via (n,p) reaction on ^{91}Zr] plotted as a function of incident neutron energy [3].

The isomeric cross-section ratio was also determined for the $^{46}Ti(n,p)^{46m,g}Sc$ process over the neutron energy range of 5.4 to 10.5 MeV. Detailed model calculations on this process were carried out (in collaboration with M. Uhl, IRK Vienna). The calculated ratio was found to be strongly dependent on the input level scheme of the product nucleus (for details cf. [4]).

1.4 Activation Cross Sections for Fusion Reactor Technology

N.I. Molla, R. Wölfle, S. Sudár, S.M. Qaim, G. Stöcklin
(Relevant to request identification numbers: 721055R, 761055R, 861113F, 861175F, 872030R, 873007R)

After completing activation cross-section measurements on fast neutron induced reactions on Mo, Nb and Zr [2,5-7], investigations were initiated on (n,p) and (n,α) reactions on isotopes of titanium. Cross sections were measured for the first time for the reactions ^{49}Ti(n,p)^{49}Sc, ^{50}Ti(n,p)^{50}Sc and ^{50}Ti(n,α)^{47}Ca from theshold up to 10.5 MeV. In the case of ^{48}Ti(n,α)^{45}Ca reaction measurements are in progress. The product was separated radiochemically and the radioactivity determined via low-level β^- counting.

Excitation functions of ^{nat}Ti(n,x)^{46,47,48}Sc processes, of relevance to neutron dosimetry, were measured in the neutron energy range of 12.5 to 20 MeV (in collaboration with H. Liskien, CBNM Geel).

Measurements were initiated on the ^{58}Ni(n,p)^{58m}Co and ^{60}Ni(n,p)^{60m}Co reactions. First results at $E_n \approx 8$ MeV show that the cross sections amount to a few mb.

Investigations were started on the ^{63}Cu(n,p)^{63}Ni, ^{151}Eu(n,2n)^{150m}Eu and ^{159}Tb(n,2n)^{158}Tb reactions under an IAEA-research agreement. These reactions lead to the formation of long-lived activation products.

2. Charged Particle Data

2.1 ^{7}Be-Emission in Proton Induced Reactions

B. Scholten, S.M. Qaim, G. Stöcklin

We investigated for the first time the excitation functions of (p,^{7}Be) reactions on ^{51}V, ^{93}Nb, ^{197}Au and ^{209}Bi in the proton energy range of 40 to 100 MeV (cf. last Progress Report). Extensive radiochemical separations were carried out to isolate ^{7}Be from the matrix activity. Thereafter the radioactivity was determined via γ-ray spectroscopy. Detailed analysis of the data is in progress.

Cross sections were also measured radiochemically for ^{7}Be-emission in the interactions of V, Nb and Au with 800, 1200 and 2600 MeV protons (for details cf. [8]).

2.2 Excitation Functions and Yields Relevant to Radioisotope Production

F. Tárkányi, Z. Kovács, M. Sajjad, S.M. Qaim, G. Stöcklin

Continuing our studies [cf. 9-11] on the production of medically important short-lived radioisotopes we measured excitation functions and yields for the formation of $^{81}Rb(^{81m}Kr)$, ^{123}I and ^{122}I. In the former case work was done under a German-Hungarian bilateral agreement. ^{nat}Kr and enriched ^{82}Kr gas cells were irradiated with protons of energy up to 30 MeV and measurements on the excitation functions of $^{82}Kr(p,n)^{82}Rb$ and $^{82}Kr(p,2n)^{81}Rb$ reactions performed. An analysis of the data is underway.

In recent years ^{123}I has been produced via the $^{124}Xe(p,x)^{123}I$-process on highly enriched ^{124}Xe. The available production yield data were discrepant and the cross-section data scanty. We measured the excitation functions of $^{124}Xe(p,2n)^{123}Cs$ and $^{124}Xe(p,pn)^{123}Xe$ reactions up to 44 MeV using 99.9 % enriched ^{124}Xe (in collaboration with H. Schweickert, KFZ Karlsruhe and R.M. Lambrecht, KFSH, Riyadh, Saudi Arabia). The results are shown in Fig. 2. The (p,2n) reaction is much stronger than the (p,pn) channel; above

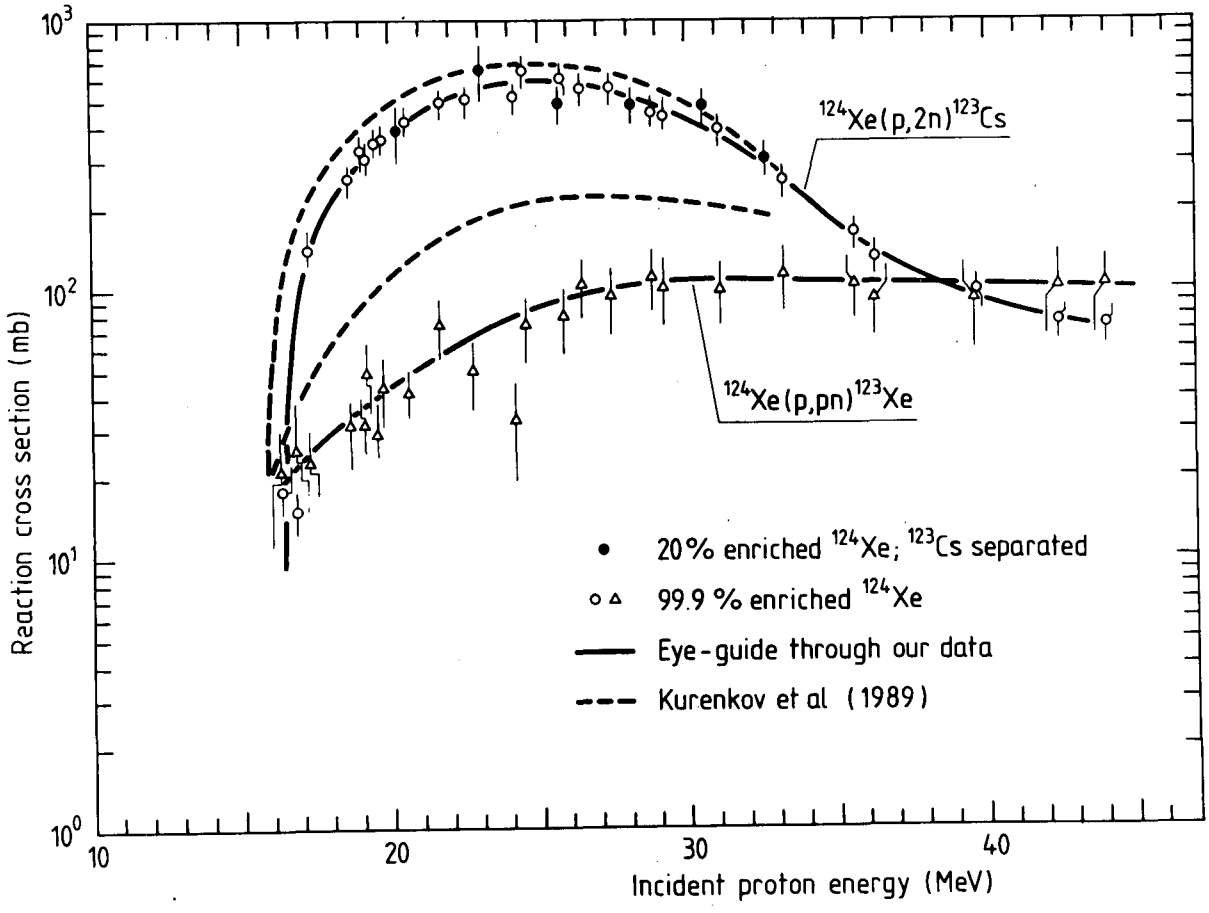

Fig. 2 Excitation functions of $^{124}Xe(p,2n)^{123}Cs$ and $^{124}Xe(p,pn)^{123}Xe$ reactions. The available literature data up to 33 MeV are also shown.

36 MeV, however, the two processes have almost equal cross sections (for details cf. [12]). Our studies show that the optimum energy range for the production of ^{123}I is $E_p = 29 \rightarrow 23$ MeV. The theoretically expected thick target yield of ^{123}I at 6.6 h after EOB amounts to 11.2 mCi/μAh.

^{122}I is a short-lived ($T_{\frac{1}{2}}$ = 3.6 min) β^+ emitting radioisotope of iodine and is produced via the $^{122}Xe \rightarrow {}^{122}I$ generator system. The parent radioisotope ^{122}Xe ($T_{\frac{1}{2}}$ = 20.1 h) is generally obtained via the $^{127}I(p,6n)$-reaction at $E_p \geq 60$ MeV. We investigated the production route $^{124}Xe(p,x)^{122}Xe$ at a medium-sized cyclotron. Excitation functions were measured for the $^{124}Xe(p,3n)^{122m}Cs$ and $^{124}Xe(p,x)^{122}Xe$ processes from threshold up to 44 MeV. The optimum energy range for the production of ^{122}Xe was found to be $E_p = 43 \rightarrow 35$ MeV. The thick target yield amounts to 13.5 mCi/μAh (for details cf. [13]).

References

[1] R. Wölfle, S.M. Qaim, H. Liskien, R. Widera: Systematic studies of excitation functions of (n,t) reactions on medium and heavy mass nuclei, Radiochimica Acta 50 (1990) 5

[2] S.M. Qaim, R. Wölfle, B. Strohmaier: First and second chance proton emission in the interactions of fast neutrons with ^{92}Mo, Phys. Rev. C40 (1989) 1993

[3] S.M. Qaim, M. Ibn Majah, R. Wölfle, B. Strohmaier: Excitation functions and isomeric cross-section ratios for the $^{90}Zr(n,p)^{90m,g}Y$ and $^{91}Zr(n,p)^{91m,g}Y$ processes, Phys. Rev. C, in press

[4] N.I. Molla, S.M. Qaim, M. Uhl: Activation cross section and isomeric cross-section ratio for the $^{46}Ti(n,p)^{46m,g}Sc$ process, Phys. Rev. C, submitted

[5] H. Liskien, R. Wölfle, R. Widera, S.M. Qaim: Excitation functions of (n,p) and (n,α) reactions on molybdenum isotopes, Appl. Radiat. Isotopes 41 (1990) 83

[6] M. Ibn Majah, S.M. Qaim: Activation cross sections of neutron threshold reactions on some zirconium isotopes in the 5.4 to 10.6 MeV energy range, Nucl. Sci. Eng. 104 (1990) 271

[7] S.M. Qaim: Neutron activation cross-section measurements on zirconium, niobium and molybdenum in the energy range of 4 to 10 MeV using radiochemical techniques, Proc. Specialists' Meeting on Neutron Activation Cross Sections for Fission and Fusion Energy Applications, Argonne, September 1989, (Edited by M. Wagner and H. Vonach) NEANDC-259 "U" (1990) p. 135

[8] R. Wölfle, S.M. Qaim: ^{7}Be emission cross sections in high energy proton induced reactions on ^{51}V, ^{93}Nb and ^{197}Au, Radiochimica Acta, in press

[9] F. Tárkányi, Z. Kovács, S.M. Qaim, G. Stöcklin: Differential production yields of ^{123}I in proton and deuteron induced reactions on natural xenon, Radiochimica Acta 47 (1989) 25

[10] F. Tárkányi, S.M. Qaim, G. Stöcklin: Excitation functions of high-energy ^{3}He- and α-particle induced nuclear reactions on natural krypton with special reference to the production of ^{82}Sr, Appl. Radiat. Isotopes 41 (1990) 91

[11] A. Mushtaq, S.M. Qaim: Excitation functions of α- and ^{3}He-particle induced nuclear reactions on natural germanium: Evaluation of production routes for ^{73}Se, Radiochimica Acta 50 (1990) 27

[12] F. Tárkányi, S.M. Qaim, G. Stöcklin, M. Sajjad, R.M. Lambrecht, H. Schweickert: Excitation functions of (p,2n) and (p,pn) reactions and differential and integral yields of ^{123}I in proton induced nuclear reactions on highly enriched ^{124}Xe, Appl. Radiat. Isotopes, submitted

[13] F. Tárkányi, S.M. Qaim, G. Stöcklin, M. Sajjad, R.M. Lambrecht: Nuclear reaction cross sections relevant to the production of the ^{122}Xe $\rightarrow$ ^{122}I generator system using highly enriched ^{124}Xe and a medium-sized cyclotron, Appl. Radiat. Isotopes, submitted

INSTITUT FÜR KERNPHYSIK, ARBEITSGRUPPE STRAHLUNGSTRANSPORT FORSCHUNGSZENTRUM JÜLICH

1. Validation Measurements of Neutrons from (p,xn) Reactions at Proton Bombarding Energies at 597 and 800 MeV

W.B. Amian, R.C. Byrd*, D.A. Clark*, P. Cloth, P. Dragovitsch, D. Filges, C.A. Goulding*, M.M. Meier*, G.L. Morgan*, C.E. Moss*

(*Los Alamos National Laboratory, NM87545, USA)

The measurements of double-differential (p,xn) cross sections were continiued at the Target 2 area of the WNR facility, where proton beams from the LAMPF linear accelerator (LINAC) are delivered at energies up to 800 MeV (see also NEANDC(E)-302U, Vol.V, June 1989).

Experimental results for validation purposes have been obtained so far for proton bombarding energies of 597 MeV /1/, and 800 MeV /1/. The data for 597 MeV at incident proton energies are analyzed. The analysis of the measurements at 800 MeV is underway.

The data were taken at 30°, 60°, 120° and 150°. At 597 MeV measurements were done for the elements Be, B, C, O, Al, Fe, Pb and U and at 800 MeV incident proton energy for the elements B, N, Al, Fe, Pb and U. Validation comparisons for the data using the KFA-version of HETC are partly published in /2/. A first example of the comparison between the KFA version of HETC and the experimental data is shown in Fig. 1 and 2 for p-induced neutron emission from a thin iron target at 597 MeV induced proton beam. In the most cases the agreement between calculated and measured data is fairly well. Some of the discrepancies have to be carefully investigated.

References

/1/ W.B. Amian, R.C. Byrd, D.A. Clark, C.A. Goulding, G.L. Morgan, C.E. Moss, to be published

/2/ P. Cloth, P. Dragovitsch, D. Filges, Ch. Reul, W.B. Amian, M.M. Meier, Intranuclear Cascade Evaporation Model Predictions of Double Differential A(p,xn) Neutron Cross Sections and Comparison with Experiments at 318 MeV and 800 MeV Proton Energy, KFA-Report Jül-2295, August 1989

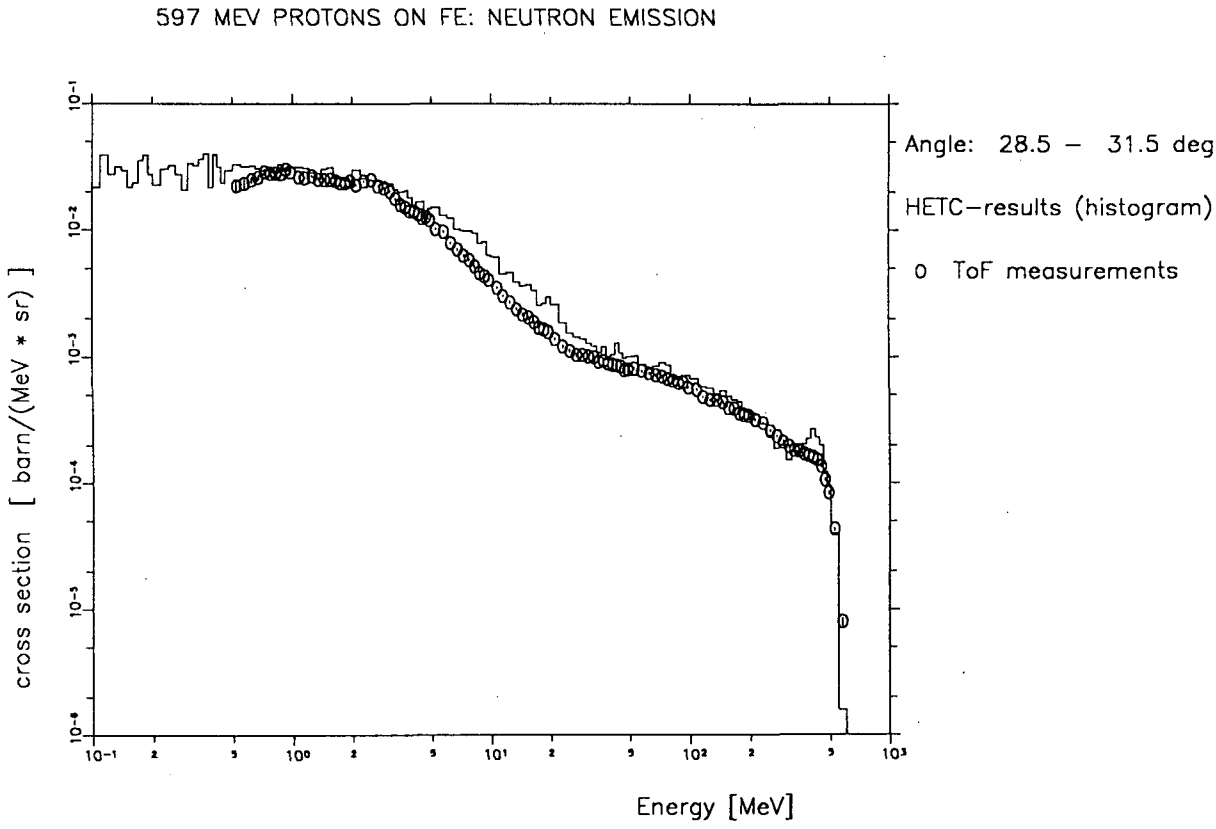

Fig. 1: Double differential cross sections of iron for neutron emission at 30° at 597 MeV incident proton energy: comparison between HETC-calculations and TOF-measurements

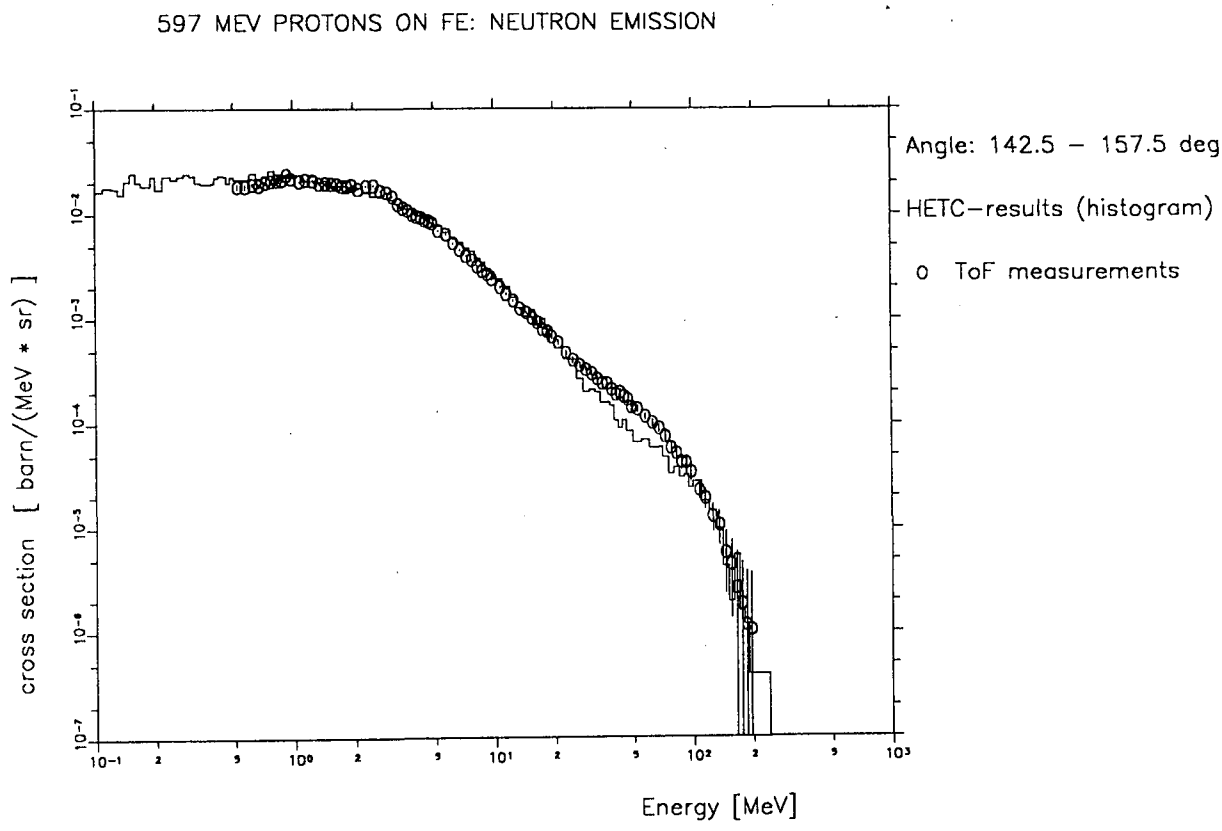

Fig. 2: Double differential cross sections of iron for neutron emission at 150° at 597 MeV incident proton energy: comparison between HETC-calculations and TOF-measurements

2. INC/E-Model Calculations of Double Differential (p,xn) Cross Sections

P. Cloth, P.Dragovitsch, D.Filges, and Ch.Reul

High resolution calculations of the proton induced neutron emission for several target nuclei and for proton energies of 113, 256, 318, 596 and 800 MeV are performed using the intranuclear cascade/evaporation model (INC/E) of the HERMES module HETC/KFA-2 /1/. The analysis of these calculations is adapted to respective experiments at the LAMPF /2/. This allows a direct comparison between measurements and model calculations at the experimental angles. Furthermore cross sections at angle ranges being not available in the experiments are calculated. The data deliver a large base for a multiparameter (A_{Target}, Z_{Target}, E_{inc}, Ω, E_n) analysis of the INC/E model.

The INC/E-Model

A detailed description of the original INC/E-model is given by several references (e.g. /3,4/ and references therein). In the present version beside the processes of intranuclear cascade and of evaporation high energy fission is allowed, too.
The INC/E-model assumes the nucleon density inside a nucleus to be Fermi-distributed as proposed by Hofstadter /5/.This is carried out in the code by partitioning the nucleus into three regions of constant nucleon density. The outer radius of each region is chosen by solving for r the density function at values of 90%, 20%, and 10% of the central density. Consequently the outest of these radii delivers the "geometric" cross section (see table 1) of the respective nucleus. The nucleon momenta are assumed to be Fermi-distributed, too. They are normalized in each region of nucleon density. The potential energies of the nucleons are estimated as the sum of the zero temperatures of the nucleons and of the binding energy of the most loosely bound nucleon.

Performing INC the incident particles are selected uniformly over the geometric cross section of the nucleus. Because the short wave length of the high energetic incident particle it is assumed that its interactions with the nucleons can be treated as free-particle collisions inside the nucleus. These

collisions are calculated using cross sections of elastic and inelastic nucleon-nucleon- and pion-nucleon scattering, cross sections for charge exchange, for single pion production, and for double pion production. If the energies of the cascade particles inside the nucleus become relatively small the cascade process is stopped. The subsequent processes are described in terms of the evaporation model EVAP /6,1/, based on the well known Weisskopf theory of evaporation. No contributions are done to a preequilibrium phase between intranuclear cascade and the evaporation phase.

target element	σ_{geom} [b]
C	0.7745
Al	1.0282
Fe	1.2676
Pb	2.4572
U_{dep}	2.6129

Table 1: "Geometric" cross sections used in the INC/E model

target element	E [MeV]	exp. angles [°]
C	113.	7.5, 30., 60., 150.
C	256.	7.5, 30., 60., 150.
C	318.	7.5, 30.
C	597.	30., 60., 120., 150.
C	800.	7.5, 30.*)
Al	113.	7.5, 30., 60., 150.
Al	256.	7.5, 30., 60., 150.
Al	318.	7.5, 30.
Al	597.	30., 60., 120., 150.
Al	800.	7.5, 30.*)
Fe	113.	7.5, 30., 60., 150.
Fe	256.	7.5, 30., 60., 150.
Fe	597.	30., 60., 120., 150.
Fe	800.	*)
Pb	113.	7.5, 30., 60., 150.
Pb	256.	7.5, 30., 60., 150.
Pb	318.	7.5, 30.
Pb	597.	30., 60., 120., 150.
Pb	800.	7.5, 30.*)
U_{dep}	113.	7.5, 30., 60., 150.
U_{dep}	256.	7.5, 30., 60., 150.
U_{dep}	318.	7.5, 30.
U_{dep}	597.	30., 60., 120., 150.
U_{dep}	800.	7.5, 30.*)

Table 2: Sets of experimental data available from /2/ for INC/E-model validations. *) still in preparation

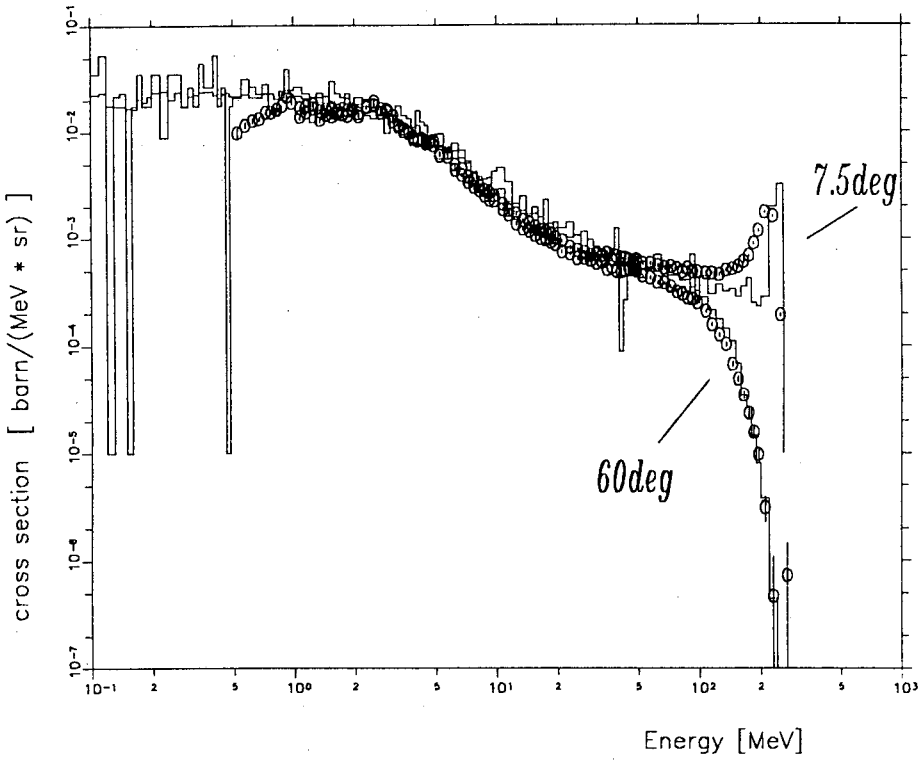

Fig. 1: $d^2\sigma/dE \cdot d\Omega$ for neutron emission from Fe at 7.5° and 60° induced by 256 MeV protons (histogram: INC/E-calculations; circles: ToF-measurements by /2/)

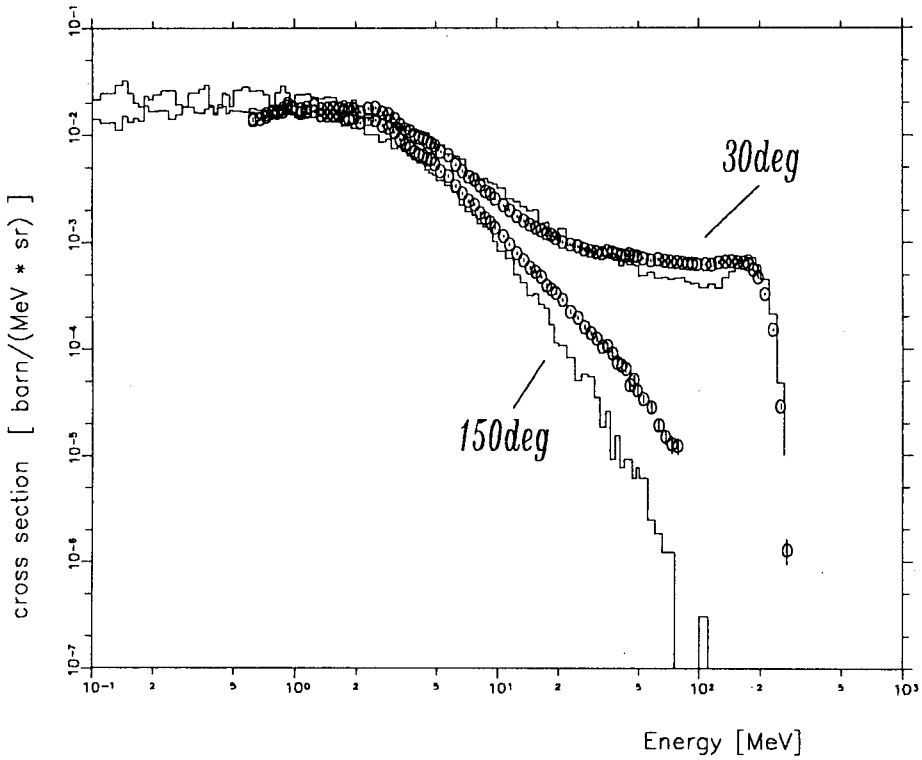

Fig. 2: $d^2\sigma/dE \cdot d\Omega$ for neutron emission from Fe at 30° and 150° induced by 256 MeV protons (histogram: INC/E-calculations; circles: ToF-measurements by /2/)

In the present INC/E model working in the HETC-module of the HERMES code system /1/ updates of the atomic masses using the 1977 Atomic Mass Evaluation values of Wapstra and Bos /7/ are included. This data are extended by the semiempirical mass formula of Cameron /8/. The level density parameter B_0 now can be taken as a function of the atomic weight A, using data compiled by Baba /9/. Furthermore the recoil momentum of the residual nucleus is considered resulting in a non-isotropic evaporation of particles in the laboratory system. At last the high energy fission model (RAL-model, /10/) basing on the statistical model of Fong /11/ is been included.

Calculational

The calculations are performed in a so called "thin target setup" of the HETC-code, in principle consisting on the pure INC/E-model of the code and the analysis modules. The calculations up to now cover the double differential proton induced neutron emission at incident energies of 113, 113, 256, 318, 596 and 800 MeV. As target elements C, Al, Fe, Pb, and depleted U (U_{dep}) are considered. Each case is calculated with high Monte-Carlo statistic of typically $5 \cdot 10^5$ to $2.5 \cdot 10^6$ simulated incident protons. The analysis covers the whole range of possible emission angles between 0° and 180°. With this a data base is created for the analysis and for the validation of the INC/E-model. Together with the measurements at LANL /2/ (table 2) a multiparameter (A_{Target}, Z_{Target}, E_{inc}, Ω, E_n) study of neutron emission in medium-energy physics is possible (e.g. Fig. 1,2). This will be helpful as for code validations as for code-extensions and -optimation.

References:

/1/ P.Cloth et al., JUEL-2203 (1988)
/2/ W.Amian et al., this report.
/3/ H.W.Bertini, Phys. Rev. 188, (1969) 1711 .
/4/ K.C.Chandler and T.W.Armstrong, ORNL-4744 (1972); Nucl. Sci. Eng. 49 (1972) 110.
/5/ R.Hofstadter, Revs. Mod. Phys. 28 (1956) 214.
/6/ V.F.Weisskopf, Phys. Rev. 52 (1937) 295; V.F.Weisskopf and H.D.Ewing, ibid. 50 (1940) 475.
/7/ H.Wapstra and K.Bos, At. Data Nucl. Data Tables 19 (1977)
/8/ A.G.W.Cameron, Ca. J. Phys. 35 (1957) 1021; ibid. 36 (1958) 1043.
/9/ H.Baba, Nucl. Phys. A159 (1970) 625,
/10/ F.Atchinson JUEL-Conf-34 (1980) 17.
/11/ P.Fong, "Statistical Theory of Nuclear Fission", Gordon and Beach Science Publishers, New York, 1969

3. A Coupled n-γ Transport Library for the Calculation of Planetary Gamma Ray Spectra Including Characteristic Gamma Ray Lines

G. Dagge, P. Dragovitsch, D. Filges

The HERMES code system /1/ was applied for a simulation of the Galactic Cosmic Ray (GCR) irradiation of a planetary (or lunar) surface. This simulation is necessary for the interpretation of gamma ray spectra from Mars, which will be provided by the gamma ray spectrometer (GRS) of the "Mars Observer". This NASA mission is scheduled for launch in 1992. Gamma rays from (n,γ) or (n,n'γ) reactions give a characteristical fingerprint of the target nucleus. Therefore, a gamma ray spectrum contains information about the amount of elements, which compose the irradiated material.

Since appropriate experimental data from Mars are not available, the Moon was chosen as a test case for the calculations. A 2π irradiation of an averaged lunar material with a realistic proton spectrum up to 10 GeV was simulated to obtain the resulting depth dependent neutron and proton fluxes. Based on the excellent agreement of calculated neutron fluxes with experimental data (e.g. /2/) a method for gamma ray production and transport was developed.

Since available group cross section libraries for coupled n-γ transport calculations with the HERMES module MORSE-CG do not include gamma ray line data, a new library was created, which has also a finer energy group structure for thermal neutrons. This library was evaluated for a variety of elements at T=293.6 K. The cross section data are stored for 118 neutron groups with an energy from 14.9 MeV to 10^{-5} eV (19 of the below 0.414 eV) and 21 gamma ray groups from 14 MeV to 10 keV. The library can be extended for several gamma ray line groups with a (rather arbitrary) width of 10 keV. The number of gamma ray lines, which can be included is not restricted but should not exceed 20 to limit the size of the library. The corresponding photon production data were evaluated from ENDF/B-IV using the AMPX system. The new library was tested for the lunar case, a comparison with Ref. /3/ showed a good overall agreement. Parallel to the Monte Carlo simulations an analyti-

cal code for production and transport of gamma ray line intensities was developed for a planar geometry, based on the simulated Monte Carlo neutron fluxes. This allows to calculate weak gamma ray line intensities within a reasonable computing time.

The procedure was applied afterwards for a typical Martian soil and atmosphere. For these calculations only minor changes in the program input had to be made. Fig. 1 shows the prompt gamma ray spectrum from a Martian surface resulting from a Monte Carlo simulation. The gamma ray spectrum from residual nuclei and from the decay of GCR-produced π^0 mesons was included in the simulations. Parameter studies concerning a variation of the chemical composition /4/ were started. As an example, the ratio of two gamma ray lines from silicon as a function of the water content of the Martian soil is presented in Fig. 2. These data were obtained analytically and can be used to determine the water content of the soil from orbital gamma ray spectra. Further parameter variations will follow.

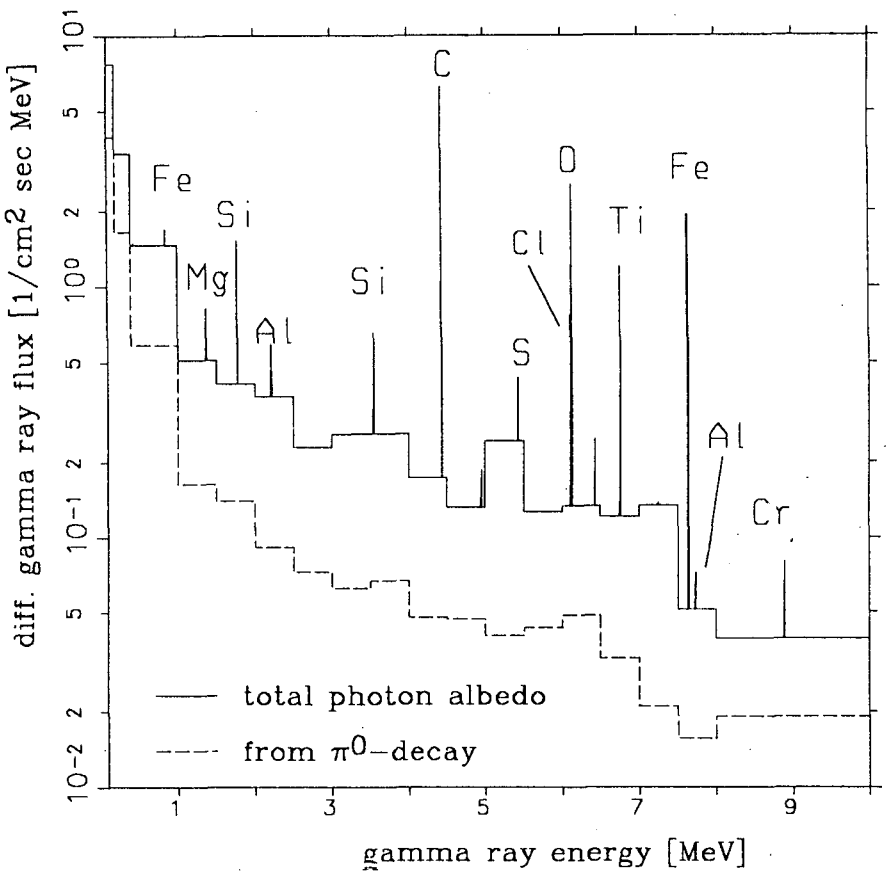

Fig. 1: Calculated prompt gamma ray spectrum of a Martian surface. Some of the most important lines were selected for the calculation.

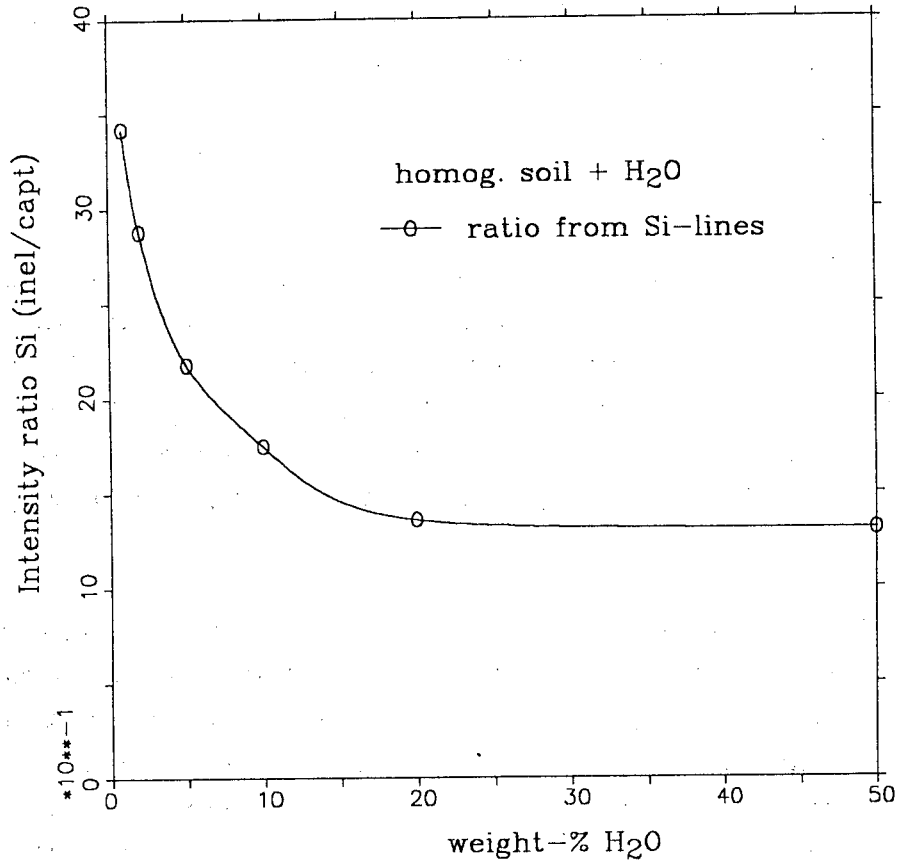

Fig. 2: Calculated ratio of the 1.779 MeV Si-line (inelastic) to the 3.539 MeV Si capture lines as a function of the water content of a homogenous Martian soil.

References:

/1/ P. Cloth, et al., HERMES, Jül-2203, May 1988

/2/ D.S. Woolum et al., The Moon 12 (1975), p. 321-350

/3/ R.C. Reedy, Proc. Lunar and Planet. Sci. Conf. 9th (1978) p. 2961-2984

/4/ L.G. Evans, J. Geophys. Res. Vol. 91, No. B9 (1987) p. 9153-9167

4. Fast Algorithm Treating Nucleon and Pion Collisions with Deuterium at Energies Between 0.02 and 2.5 GeV

P. Dragovitsch

Phase space models (PSM) provide the state of all particles produced in noneleastic nuclear collisions by considering the density of states produced over the total allowable particle phase space. An approach is presented treating the collisions of p, n, π^+, and π^- with deuterium in the energy range between 20 MeV and 2.5 GeV for applications of high energy particle transport problems.

In principle, PSM-models are rather straightforward in that the state density of outcomes can be determinated from first principles and the kinematics of the reaction. With respect to the idea of fast computing the PSM is very applicable for deuterium as target nucleus. Basic concept of PSM is the description of the state of motion for any particle as a point in the six dimensional phase space defined by its position **x** and momentum **p**. The uncertainty relation requires a seperation of these coodinates into finite distances:

$$dx_i \cdot dp_i \geq 2\pi\hbar.$$

This leads in consequence to the Lorentz invariant form of the phase space integral

$$\frac{dN_n}{dE} = R_n(0,E) = \int \prod_{j=1}^{n} \frac{d^3p_j}{2E_j} \; \delta^3 \left[\sum_{i=1}^{n} p_i\right] \cdot \delta\left[\sum_{i=1}^{n} E_i - E\right]$$

which can be solved easily for the two particle phase space. Using the recursion formula of Srivastava and Sudershan /1/

$$R_n(0,E) = \int \frac{d^3p_n}{2E_n} R_{n-1}(0,\mu) \; ; \quad \mu = [(E-E_n)^2 - (\ -p_n)^2]^{\frac{1}{2}}$$

a way is found write the phase space integral for arbitrary n's. The numerical approach to solve the integral is to use the invariant mass distributions, where the invariant mass of k particles labeled i....j in a n particle system is defined by ${}^{n}M_k{}^2=(E_i+ \ldots +E_j)^2 - (p_i+ \ldots+p_j)(p_i + \ldots p_j)$.

In this manner the invariant n-body integral can be transformed into terms of two particle break ups and than can be solved with Monte Carlo methods using an unique distribution over the invariant masses.

Each of these two-body reactions is performed in the repective CM system. By assuming isotropic decay and keeping track of each system transformation and rotation the final state energy and direction in the laboratory frame is obtained for each particle. Since one has not sampled the invariant mass each event must be assigned a weight according to the value of the integrand. After playing this procedure n-times with sufficient statistics the final statistical weight of a particle is reached by dividing its individual weight through the total sum of weights resulting in a normalization to a reaction rate of 1.
To extend these formalism for a quantitative description of nucleon- and/or pion-collisions with deuterium in an application as a single event generator it has to be extended by using nucleon-nucleon cross sections and nucleon-pion cross sections (see /2/ and references therein) delivering the probability for the respective final state configurations. In addition, precomputed energy dependend phase space volumes are included to accelerate the algorithm.

In the actuell version the model is able to treat incident particles as protons, neutrons, π^+, and π^-, delivering outcoming particles as protons, neutrons, π^+, π^0, and π^-, together with the information of their momentum, energy, and statistical weight. For an implementation in a transport code the options are given to use a static external "geometric" cross section (like in the HETC /2/) or to use a total cross section calculated internally.
Beside its application as an event generator in high energy transport codes the model is able to predict differential (e.g. Fig. 1) and double differential cross sections for the emission of the individual outcoming particles.

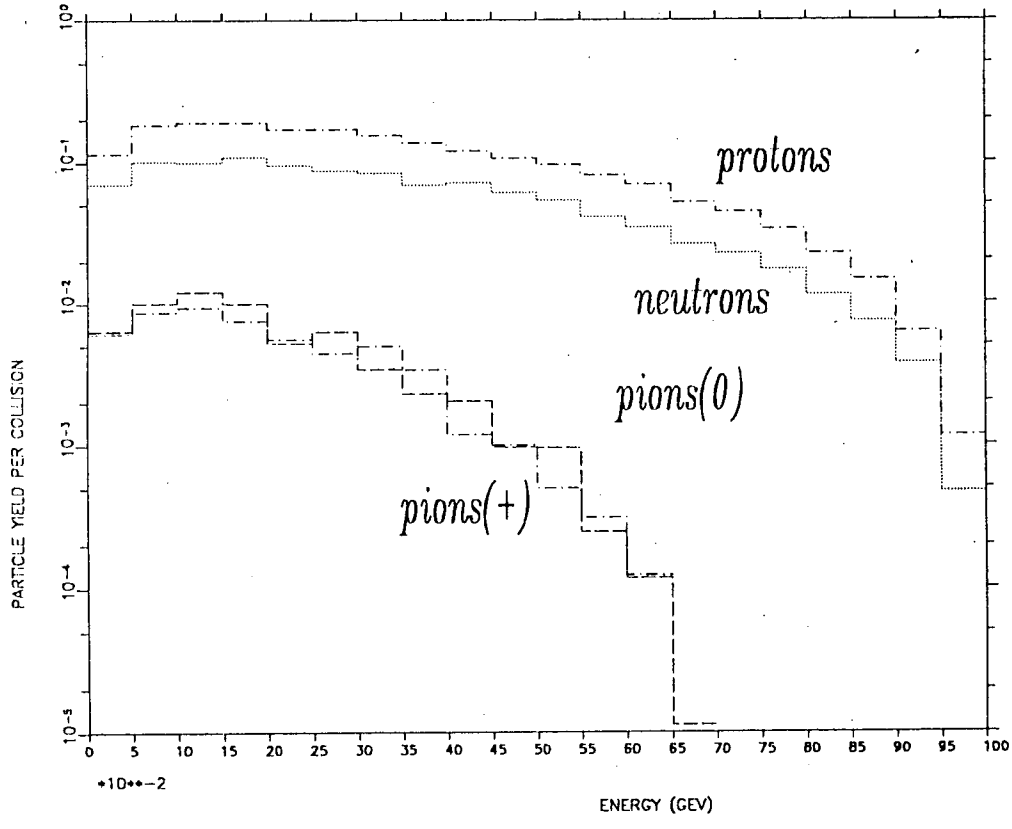

Fig.1: 1 GeV protons on deuterium: calculated yields per collision of protons, neutrons, π^+, and π^0.

In principle the algorithm can be extended to other collisions with dibaryons. An interesting application would be a its use within an intranuclear cascade model for treating many-body collisions at medium or minor energies inside the nucleus itself.

References:

/1/ P.P.Srivastava and G.Sudershan,(1958) Phys.Rev.110, 765.
/2/ P.Cloth et al., (1988), JÜL-2203

INSTITUT FÜR KERNPHYSIK, EXPERIMENTELLE KERNPHYSIK II FORSCHUNGSZENTRUM JÜLICH

1. Determination of Lifetimes of Levels in ^{96}Zr

H. Ohm[a], M. Liang[a], G. Molnar[a,b], S. Raman[c], K. Sistemich[a], W. Unkelbach[a]

Laboratories:
a) Forschungszentrum Jülich, Institut für Kernphysik, Postfach 1913, D–5170 Jülich, F.R. Germany
b) Institute of Isotopes, H–1525 Budapest, Hungary
c) Oak Ridge National Laboratory, Oak Ridge, Tennessee 37831, USA

Names: H. Ohm (a), M. Liang (a), G. Molnár (a,b), S. Raman (c), K. Sistemich (a), W. Unkelbach (a)

Facilities: Fission–product separator JOSEF (Reactor DIDO, Jülich)

Experiment: Determination of lifetimes of the 3_1^- state at 1897 keV ($t_{1/2} = 46 \pm 15$ ps) and of the 8_1^+ state at 8390 keV ($t_{1/2} = 127 \pm 10$ ps) in ^{96}Zr. Deduced unusually high octupole collectivity of B(E3: $3_1^- \rightarrow 0^+$) = 69^{+34}_{-17} spu and weak quadrupole collectivity of B(E2: $8_1^+ \rightarrow 6_2^+$) = 1.4 ± 0.1 spu.

Method: Separation of fission products according to their masses and nuclear charges. Measurement of delayed $\beta\gamma\gamma$ coincidences. Fast timing with plastic and BaF_2 scintillation detectors.

Accuracy:

Completion: Partly completed

Publication: Phys. Rev. Lett. B, in print
Annual Report 1989, IKP Forschungszentrum Jülich, p. 32, in print

2. Identification and Spin Assignment of Levels in ^{96}Zr up to 4640 keV Excitation Energy

G. Molnar[a,b], J. Hebenstreit[a,c], S. Heising[a], P. Maier-Komor[d], H. Ohm[a], D. Paul[a], P. von Rossen[a], K. Sistemich[a], W. Unkelbach[a]

Laboratories:

a) Forschungszentrum Jülich, Institut für Kernphysik, Postfach 1913, D–5170 Jülich, F.R. Germany
b) Institute of Isotopes, H–1525 Budapest, Hungary
c) Institute of Physics, Jagellonian University, Cracow, Poland
d) Physik–Department, Technische Universität München, D–8046 Garching

Names: G. Molnar (a,b), J. Hebenstreit (a,c), S. Heising (a), P. Maier–Komor (d), H. Ohm (a), D. Paul (a), P. von Rossen (a), K. Sistemich (a), W. Unkelbach (a)

Facilities: Isochronous Cyclotron JULIC, magnetic spectrometer Big Karl, Jülich

Experiment: Identification and spin assignment of levels in ^{96}Zr up to 4640 keV excitation energy.

Method: ^{96}Zr (d,d') inelastic scattering with E_d = 52 MeV. Analysis of scattered particles in magnetic spectrometer. Measurement of angular distributions and DWBA analysis.

Accuracy: Energy resolution: 14 ± 2 keV

Completion: work in progress

Publication: Annual Report 1989, p. 1, IKP–Forschungszentrum Jülich, in print

3. Determination of Lifetimes of Levels in ^{99}Nb

H. Ohm

Laboratory:	Forschungszentrum Jülich, Institut für Kernphysik, Postfach 1913, D–5170 Jülich, F.R. Germany
Names:	H. Ohm
Facilities:	Fission–product separator JOSEF (Reactor DIDO, Jülich)
Experiment:	Determination of lifetimes of levels in ^{99}Nb. Deduced B(E2) values. Identification of members of $2^+ \otimes \pi g_{9/2}$ multiplet.
Method:	Separation of fission products according to their masses and nuclear charges. Measurement of delayed $\beta\gamma\gamma$ coincidences. Fast timing with plastic and BaF_2 scintillation detectors.
Accuracy:	Uncertainty of measured half–lives $\leq$ 10 ps
Completion:	work in progress
Publication:	Annual Report 1989 IKP–Forschungszentrum Jülich, p. 34, in print

4. Determination of the Lifetime of a (4^+) Level in ^{100}Zr

H. Ohm, M. Liang, G. Molnár, K. Sistemich

Laboratory: Forschungszentrum Jülich, Institut für Kernphysik, Postfach 1913, D–5170 Jülich, F.R. Germany

Names: H. Ohm, M. Liang, G. Molnár (on leave of absence from the Institute of Isotopes, Budapest/Hungary), K. Sistemich

Facilities: Fission–product separator JOSEF (Reactor DIDO, Jülich)

Experiment: Determination of $t_{1/2}$ (4^+) = (37 ± 4) ps in ^{100}Zr. Deduced ground–state deformation $\beta = 0.30 \pm 0.02$.

Method: Separation of fission products according to their masses and nuclear charges. Measurement of delayed $\beta\gamma\gamma$ coincidences. Fast timing with plastic and BaF_2 scintillation detectors.

Accuracy:

Completion: Completed

Publication: Z. Phys. A334, 519 (1989)

5. Determination of Level Lifetimes in the Deformed Nuclei ^{101}Nb, ^{103}Mo and ^{104}Mo

M. Liang[a], H. Ohm, K. Kawade[d], G. Molnár[a,b], U. Paffrath[a], T. Seo[c], B. de Sutter[a], K. Sistemich[a]

Laboratories:

a) Forschungszentrum Jülich, Institut für Kernphysik, Postfach 1913, D–5170 Jülich, F.R. Germany
b) Institute of Isotopes, H–1525 Budapest, Hungary
c) Research Reactor Institute, Kyoto University, Osaka, 590–04, Japan
d) Faculty of Engineering, Nagoya University, Nagoya, 464, Japan

Names: M. Liang (a), H. Ohm (a), K. Kawade (d), G. Molnár (a,b), U. Paffrath (a), T. Seo (c), B. de Sutter (a), K. Sistemich (a)

Facitilies: Fission–product separator JOSEF (Reactor DIDO, Jülich)

Experiment: Determination of level lifetimes in the deformed nuclei ^{101}Nb, ^{103}Mo and ^{104}Mo. Deduced $|Q_0|$ and $|\beta|$ for rotational levels. Evidence for strong and nearly constant ground state deformation for $N \geq 60$.

Method: Separation of fission products according to their masses and nuclear charges. Measurement of delayed $\beta\gamma\gamma$ coincidences. Fast timing with plastic and BaF_2 scintillation detectors.

Accuracy: varying; examples:
$t_{1/2}$ (^{100}Zr, 564 keV level) = (37 ± 4) ps
$t_{1/2}$ (^{101}Nb, 206 keV level) = (1.82 ± 0.04) ns.

Completion: Partly completed

Publication: Annual Report 1989, IKP Forschungszentrum Jülich, p. 38, 40 and 42, in print

GKSS-FORSCHUNGSZENTRUM GEESTHACHT GMBH
INSTITUT FÜR PHYSIK

14 MeV Neutron Activation Cross Sections of Cu and Ag

R. Pepelnik, H.M. Agrawal*, E. Bössow, J. Csikai**, Cs.M. Buczko**

Fast neutron cross sections are important for the estimation of radioactive waste and nuclear heating of materials to be used in fusion reactors.

Pure metallic foils were irradiated with 10^{14} n/cm² at the KORONA neutron generator facility [1] within approximately 2 hours. The activities have been measured in Debrecen and Geesthacht [2]. Cross sections for producing long-lived isotopes in Cu and Ag were determined (see Table I).

Employing the well known excitation function of the reactions ^{90}Zr(n,2n) [3] and ^{93}Nb(n,2n) [4] the neutron energy at the centre of the cylindrical target of KORONA was determined to 14.5 ± 0.3 MeV.

Table I Activation Cross-Sections at 14.5 ± 0.3 MeV

Reaction	Half Life	Isotop. Abund. (%)	This Work 14.6±0.3 MeV (mbarn)	Literature Values 14.5 - 14.8 MeV (mbarn)	(mbarn)
^{63}Cu(n,α)^{62}Co	5.271 a	69.17	48 ± 2	35- 50 [5]	
^{107}Ag(n,2n)^{106m}Ag	8.46 d	51.84	561 ± 20	550-600 [5]	560±10[6]
^{109}Ag(n,2n)^{108m}Ag	127.7^{+} a	48.16	242 ± 20^{+}	27 [7]	·

$^{+}$According to a recent measurement [8] the half-life of ^{108m}Ag is 250 ± 50 a. This would result in a cross-section of 476 ± 39 mb.

References

[1] H.-U. Fanger, R. Pepelnik, W. Michaelis, J. Radioanal. Chem. 61 (1981) 147.
[2] J. Csikai, Cs.M. Buczko, R. Pepelnik, H.M. Agrawal, INDC(NDS)-232/L (1990) 61.
[3] A. Pavlik, G. Winkler, H. Vonach et al., J. Phys. G 8 (1982) 1283.
[4] T.B. Ryves, Ann. Nucl. Energy 16 (1989) 307.
[5] V. McLane, Ch.L. Dunford, Ph.F. Rose, Neutron Cross Sections, Vol. 2 (1988) Acad. Press, San Diego.
[6] W. Mannhart, H. Vonach, Z. für Physik A 272 (1975) 279.
[7] V.M. Bychkov et al., Cross sections for neutron induced threshold reactions, Energoizdat, Moscow (1982).
[8] W. Mannhart, private communication.

* Depart. Physics, G.B. Pant Univ., Pantnagar, India,
**Inst. Exp. Physics, Kossuth Univ., Debrecen, Hungary

ABTEILUNG NUKLEARCHEMIE
UNIVERSITÄT ZU KÖLN
AND
ZENTRALEINRICHTUNG FÜR STRAHLENSCHUTZ
UNIVERSITÄT HANNOVER

1. Cross Sections for the Production of Residual Nuclides by Proton-Induced Spallation up to 2600 MeV

B. Dittrich[1], U. Herpers[1], R. Bodemann[2], M. Lüpke[2], R. Michel[2], P. Signer[3], R. Wieler[3], H.J. Hofmann[4], W. Wölfli[4]

The knowledge of integral excitation functions for the production of residual nuclides by high-energy proton- and alpha-induced reactions is of high interest in various fields of science. In particular, they are needed in astrophysics and meteoritics to describe the interactions of cosmic rays with matter. Galactic and solar cosmic rays consist of about 90% protons and 10% alpha-particles. Stable and radioactive nuclides produced by nuclear interactions of cosmic rays with terrestrial and extraterrestrial matter - the so-called cosmogenic nuclides - give information about various processes in the solar system. For the interpretation of the production of cosmogenic nuclides in extraterrestrial matter in terms of the irradiation history of the irradiated matter or of the history of the solar and galactic radiation, exact models are required, which can be only developed on the basis of accurate cross sections of the underlying nuclear reactions in the entire energy-region of cosmic rays. For galactic particles energies between 500 MeV/A and 10 GeV/A are of interest. At the same time, excitation functions of nuclear reactions are of interest in the energy range mentioned for basic nuclear physics in order to understand nuclear reaction mechanisms, in particular the transition from preequilibrium reactions to spallation and fragmentation.

1 Abteilung Nuklearchemie, Universität zu Köln, F.R.G.
2 Zentraleinrichtung für Strahlenschutz, Universität Hannover, F.R.G.
3 Inst. für Kristallographie und Petrographie, ETH Zürich, Switzerland
4 Institut für Mittelenergiephysik, ETH Zürich, Switzerland

A survey through literature [1-5] shows that many experimental data reported in the past suffer from severe lack of accuracy. Uncertainties of up to one order of magnitude are often found when looking for non-evaluated experimental data. Such uncertainties do neither allow for stringent tests of nuclear reaction models, nor are they tolerable for the various applications of high-energy cross sections. In order to improve this situation, a number of investigations were carried out by our group during the last years, e.g. [6 - 8]. The present status of this work is described here.

1.1 Production of Short- and Medium-Lived Radionuclides by Proton-Induced Spallation between 800 and 2600 MeV

Thin-target cross sections for the production of stable and radioactive nuclides by proton-induced reactions on O, Mg, Al, Si, Ca, Ti, V, Mn, Fe, Co, Ni, Cu, Zr, Rh, Ba, and Au were determined at 800, 1200 and 2600 MeV using accelerators at LANL/Los Alamos and at LNS/Saclay. Gamma- and X-spectrometry as well as conventional and accelerator mass spectrometry are used to measure the residual nuclides, a work which is done in collaboration of groups from Köln, Hannover, and Zürich. Final results are presented for short- and medium-lived nuclides for target elements from oxygen to vanadium. First measurements by accelerator mass spectrometry (section 1.2) and by conventional mass spectrometry (section 1.3) are also now available. However, the measurements as well as the data evaluation are not yet finished in all cases. These results will be reported later.

Details about the experimental procedure will be published shortly [9,10]. The proton fluxes were determined on the basis of the cross sections for the reaction $^{27}Al(p,3p3n)^{22}Na$ as recommended by Tobailem and de Lassus St. Genies [11]. The actual cross sections adopted for this reaction were 15.5 mb, 14.4 mb, and 11.6 mb at 800 MeV, 1200 MeV, and 2600MeV, respectively. Gamma-energies, branching ratios and half-lifes of the radionuclides, which were used for the evaluation of cross sections, were taken from [12, 13]. A detailed discussion of the errors of cross section determination is given elsewhere [8, 9].

The new data, together with those reported for a proton energy of 600 MeV [8, 14], represent a consistent data set of thin-target cross sections of more than 300 individual spallation reactions. In table 1 the results obtained for target elements from oxygen to vanadium are

presented. Data for the target element iron were given in last year's progress report [15]. Together with the data for proton energies up to 200 MeV measured earlier by our group [6,7, and references therein] they give fairly complete excitation functions from the thresholds up to 2600 MeV.

Based on the new data a comparison with several calculated cross sections is presently being performed. The theoretical discussion comprises tests of the applicability of semiempirical formulae [16] as well as more physical approaches as INC/E-calculations using the HERMES code system [17] and the hybrid model [18] of preequilibrium reactions in the form of the code ALICE LIVERMORE 87 [19]. The goal of these theoretical studies is to describe the transition from preequilibrium to spallation and fragmentation [9, 10]. As a phenomenological example the dependences on target masses of the production of ^{7}Be and ^{22}Na are shown in Fig. 1 for a p-energy of 800 MeV. These data strikingly demonstrate the differences in the production modes of these two nuclides, ^{7}Be being produced by fragmentation, the production being fairly independent from target mass, while ^{22}Na shows the typical behaviour of a "deep-spallation" product with an exponential decrease of its production with increasing target mass. A detailed discussion of these aspects is given elsewhere [9].

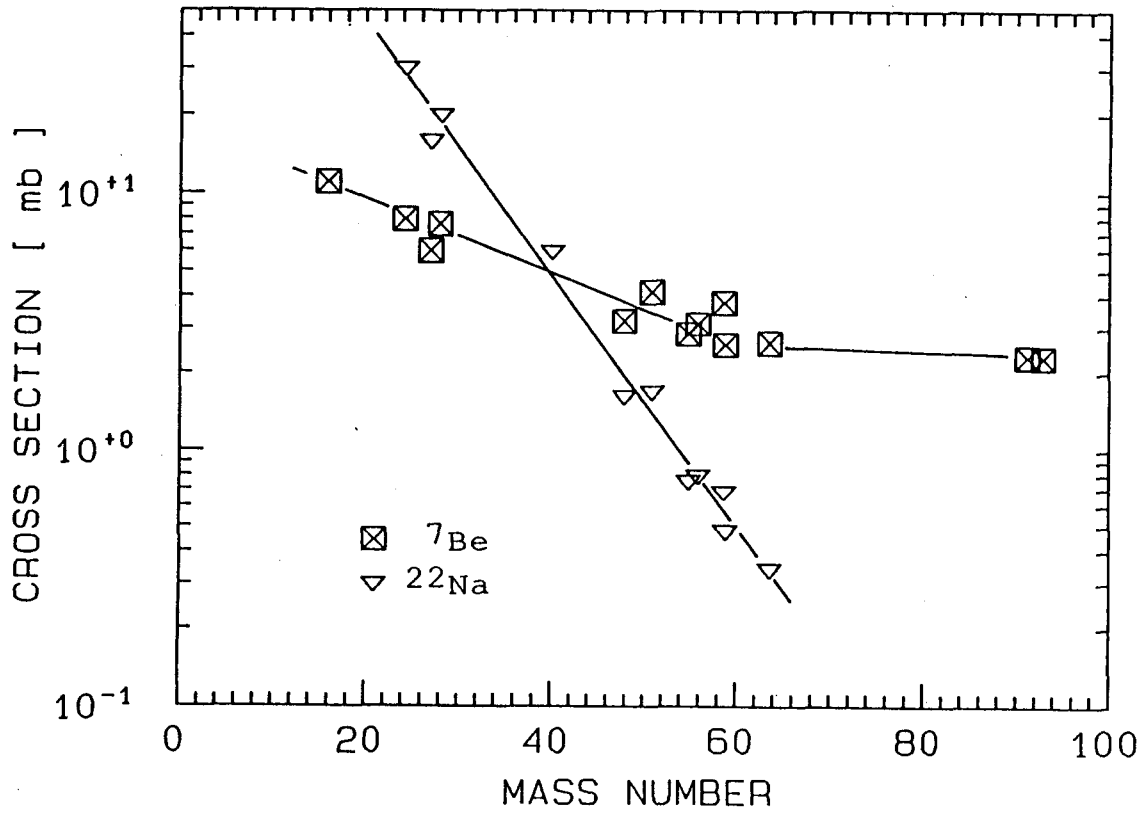

Fig. 1: Dependence on target mass of the production of ^{7}Be and ^{22}Na by 800 MeV protons.

Tab. 1: Cross sections for the production of short- and medium-lived radionuclides from oxygen, magnesium, aluminum, silicon, calcium, titanium, and vanadium by high-energy protons.

Reaction	Cross sections [mb] at a proton-energy of 800 MeV	1200 MeV	2600 MeV
O(p,5pXn)^{7}Be	11.0 ± 0.9	11.7 ± 0.9	9.41 ± 0.75
Mg(p,9pXn)^{7}Be	7.88 ± 0.64	9.92 ± 0.74	9.82 ± 0.71
Mg(p,2pXn)^{22}Na	29.7 ± 2.1	28.9 ± 2.1	23.7 ± 1.7
Mg(p,2pXn)^{24}Na		7.68 ± 0.54	7.47 ± 0.54
Al(p,10p11n)^{7}Be	5.98 ± 0.43	8.36 ± 0.61	8.65 ± 0.62
Al(p,3p3n)^{22}Na	15.6 ± 1.1	14.6 ± 1.0	11.4 ± 0.8
Al(p,3pn)^{24}Na	12.9 ± 0.9	12.0 ± 0.9	10.9 ± 0.8
Si(p,11pXn)^{7}Be	7.57 ± 0.62	10.1 ± 0.7	10.8 ± 0.8
Si(p,4pXn)^{22}Na	19.6 ± 1.4	18.9 ± 1.3	14.5 ± 1.0
Si(p,4pXn)^{24}Na	5.73 ± 0.42	5.40 ± 0.38	4.97 ± 0.36
Si(p,3p)^{28}Mg		0.0858 ± 0.0078	0.0825 ± 0.0079
Ca(p,10pXn)^{22}Na	5.87 ± 0.44	7.14 ± 0.53	5.92 ± 0.45
Ca(p,10pXn)^{24}Na	2.93 ± 0.24	3.19 ± 0.23	2.99 ± 0.22
Ca(p,9pXn)^{28}Mg		0.118 ± 0.010	0.111 ± 0.010
Ca(p,2pXn)^{42}K		0.819 ± 0.081	0.788 ± 0.072

Tab. 1: (continued) Cross sections for the production of short- and medium-lived radionuclides from oxygen, magnesium, aluminum, silicon, calcium, titanium, and vanadium by high-energy protons.

Reaction	Cross sections [mb] at a proton-energy of 800 MeV	1200 MeV	2600 MeV
$Ca(p,2pXn)^{43}K$	0.859 ± 0.064	0.816 ± 0.058	0.711 ± 0.052
$Ca(p,pXn)^{47}Ca$	0.202 ± 0.015	0.216 ± 0.016	0.199 ± 0.015
$Ca(p,Xn)^{44m}Sc$	0.0131 ± 0.0014	0.0137 ± 0.0013	0.0154 ± 0.0015
$Ca(p,Xn)^{46}Sc$	0.0294 ± 0.0045	0.0118 ± 0.0011	0.0099 ± 0.0021
$Ca(p,Xn)^{48}Sc$		0.0087 ± 0.0011	
$Ti(p,19pXn)^{7}Be$	3.19 ± 0.24	4.80 ± 0.37	6.94 ± 0.54
$Ti(p,12pXn)^{22}Na$	1.60 ± 0.12	2.64 ± 0.19	3.04 ± 0.25
$Ti(p,12pXn)^{24}Na$	2.15 ± 0.37	3.24 ± 0.23	4.62 ± 0.33
$Ti(p,11pXn)^{28}Mg$		0.431 ± 0.036	0.567 ± 0.045
$Ti(p,4pXn)^{42}K$		8.12 ± 0.61	8.33 ± 0.63
$Ti(p,4pXn)^{43}K$	4.39 ± 0.32	3.55 ± 0.25	3.48 ± 0.25
$Ti(p,3pXn)^{47}Ca$	0.332 ± 0.025	0.331 ± 0.024	0.296 ± 0.023
$Ti(p,2pXn)^{44m}Sc$	7.35 ± 0.53	6.34 ± 0.45	5.23 ± 0.37
$Ti(p,2pXn)^{46}Sc$	34.2 ± 2.4	33.8 ± 2.5	28.1 ± 2.0
$Ti(p,2pXn)^{47}Sc$	31.0 ± 2.2	29.5 ± 2.1	25.4 ± 1.8
$Ti(p,2pXn)^{48}Sc$	3.48 ± 0.25	3.42 ± 0.24	3.23 ± 0.23

Tab. 1: (continued) Cross sections for the production of short- and medium-lived radionuclides from oxygen, magnesium, aluminum, silicon, calcium, titanium, and vanadium by high-energy protons.

Reaction	Cross sections [mb] at a proton-energy of 800 MeV	1200 MeV	2600 MeV
$Ti(p,Xn)^{48}V$	1.77 ± 0.13	1.99 ± 0.15	1.99 ± 0.15
$V(p,20pXn)^{7}Be$	4.14 ± 0.32	5.98 ± 0.44	6.58 ± 0.59
$V(p,13pXn)^{22}Na$	1.67 ± 0.12	2.42 ± 0.17	2.62 ± 0.26
$V(p,13pXn)^{24}Na$		3.56 ± 0.26	4.67 ± 0.35
$V(p,12pXn)^{28}Mg$		0.487 ± 0.047	0.694 ± 0.062
$V(p,5pXn)^{42}K$		8.39 ± 0.74	8.15 ± 0.75
$V(p,5pXn)^{43}K$	4.82 ± 0.40	4.03 ± 0.29	3.67 ± 0.27
$V(p,4pXn)^{47}Ca$	0.534 ± 0.041	0.520 ± 0.040	0.487 ± 0.040
$V(p,3pXn)^{44m}Sc$	8.97 ± 0.64	7.18 ± 0.51	5.58 ± 0.40
$V(p,3pXn)^{46}Sc$	24.0 ± 1.7	22.6 ± 1.6	17.8 ± 1.3
$V(p,3pXn)^{47}Sc$	16.5 ± 1.2	14.6 ± 1.0	13.0 ± 0.9
$V(p,3pXn)^{48}Sc$	5.69 ± 0.41	5.24 ± 0.37	4.91 ± 0.36
$V(p,pXn)^{48}V$	12.6 ± 0.9	11.1 ± 0.8	9.99 ± 0.73
$V(p,Xn)^{48}Cr$		0.049 ± 0.011	
$V(p,Xn)^{51}Cr$	2 .82 ± 0.29	3.15 ± 0.24	3.02 ± 0.36

1.2 Integral Excitation Functions for the Production of Long-Lived ^{10}Be and ^{26}Al by Proton-Induced Reactions

The long-lived radionuclides ^{10}Be (T = 1.5 Ma) and ^{26}Al (T = 720 ka) are observed as cosmogenic nuclides in terrestrial and extraterrestrial materials. They are of particular interest in cosmochemistry and -physics, because they allow for the determination of irradiation ages of extraterrestrial bodies. Moreover, the cross sections for the production of these two nuclides are the key quantities to evaluate the long-term flux and spectral composition of solar cosmic ray protons from measured ^{10}Be and ^{26}Al depth profiles in lunar rocks. Here, we report on measurements of cross sections for these nuclides by accelerator mass spectrometry. The targets processed in this work originate from irradiations at CERN [14, 20], LNS/Saclay (cmp. section 1.1), LANL/Los Alamos (cmp. section 1.1), IPN/Orsay [7, 8] and Uppsala (cmp. section 2).

The chemical separations and preparations of samples for the accelerator mass spectrometry were done so, that as many long-lived radionuclides as possible were separated from each foil. Besides for ^{10}Be and ^{26}Al, samples for the determination of ^{41}Ca and ^{53}Mn were prepared, which still wait for AMS-measurement. The chemical separations consisted of a combiniation of ion exchange procedures, hydroxide precipitations and, in case of iron, solvent extractions. At the end of the separations the Be- resp. the Al-fractions were precipitated as hydroxides, washed with bidistilled water and glowed to the respective oxides. The oxide powders were mixed with high purity copper powder and pressed in sample holders for the AMS-measurements. More details about the chemical separations may be found elsewhere [21].

Here we report cross sections for the production of ^{10}Be from the target elements oxygen, magnesium, aluminum, silicon, manganese, iron and nickel (table 2) for proton-energies from reaction thresholds up to 2600 MeV. For the production of ^{26}Al final data are available now for the target elements aluminum, manganese, iron, and nickel in the same energy range (table 3). The new data fill some gaps in existing excitation functions and resolve several earlier existing discrepancies in the shapes of the excitation functions. Also hitherto unknown excitation functions were determined. A detailed description and discussion will be published elsewhere [9, 22].

Tab. 2: Experimental cross sections for the production of ^{10}Be from O, Mg, Al, Si, Mn, Fe, and Ni by high-energy protons.

E ± dE [MeV]	σ ± dσ [mb]
O(p,5pxn)^{10}Be	
52.6 ± 1.8	0.0630 ± 0.0098
68.1 ± 1.6	0.365 ± 0.049
93.4 ± 1.7	0.397 ± 0.048
96.7 ± 1.0	0.568 ± 0.064
600.	2.09 ± 0.14
800.	2.77 ± 0.17
1200.	3.44 ± 0.21
2600.	2.55 ± 0.15
Mg(p,9pxn)^{10}Be	
66.0 ± 0.7	0.0179 ± 0.0065
95.0 ± 0.2	0.0847 ± 0.0097
600.	1.11 ± 0.04
800.	1.96 ± 0.12
1200.	2.45 ± 0.15
2600.	2.89 ± 0.17
^{27}Al(p.10p8n)^{10}Be	
66.7 ± 0.8	0.0183 ± 0.0016
80.0 ± 0.3	0.0463 ± 0.0024
95.5 ± 0.2	0.0911 ± 0.0080
155.3 ± 1.1	0.162 ± 0.007
202.0 ± 1.4	0.279 ± 0.017
600.	1.33 ± 0.04
800.	2.10 ± 0.13
1200.	3.01 ± 0.18
2600.	3.02 ± 0.18
Si(p,11pxn)^{10}Be	
50.0 ± 1.4	0.0062 ± 0.0009
68.2 ± 1.2	0.0190 ± 0.0024
94.6 ± 0.5	0.0250 ± 0.0021
96.9 ± 0.7	0.0303 ± 0.0031
600.	0.640 ± 0.037
800.	1.39 ± 0.08
1200.	2.02 ± 0.13
2600.	2.38 ± 0.14
^{55}Mn(p,22p24n)^{10}Be	
63.5 ± 1.0	0.0194 ± 0.0087
93.1 ± 0.5	0.0475 ± 0.0145
115.0 ± 1.7	0.0442 ± 0.0117
132.0 ± 1.6	0.0649 ± 0.0085
171.0 ± 1.7	0.071 ± 0.014
188.0 ± 1.6	0.071 ± 0.014
600.	0.854 ± 0.043
800.	1.40 ± 0.09
1200.	2.59 ± 0.15
2600.	4.42 ± 0.25
Fe(p,23pxn)^{10}Be	
61.7 ± 1.1	0.008 ± 0.003
73.7 ± 0.5	0.024 ± 0.012
91.7 ± 0.6	0.0194 ± 0.0037
125.0 ± 1.6	0.0224 ± 0.0012
161.0 ± 1.8	0.0320 ± 0.0029
189.0 ± 1.6	0.0450 ± 0.0023
600.	0.579 ± 0.024
800.	1.03 ± 0.06
1200.	1.86 ± 0.11
2600.	3.45 ± 0.21
Ni(p,25pxn)^{10}Be	
57.2 ± 1.1	0.0035 ± 0.0015
88.4 ± 0.6	0.0081 ± 0.0024
115.0 ± 1.6	0.0235 ± 0.0063
132.0 ± 1.5	0.0198 ± 0.0024
148.0 ± 1.4	0.0285 ± 0.0030
166.0 ± 1.7	0.0290 ± 0.0056
188.0 ± 1.5	0.0209 ± 0.0033
600.	0.428 ± 0.016
800.	0.762 ± 0.030
1200.	1.45 ± 0.06
2600.	2.91 ± 0.11

Tab. 3: Experimental cross sections for the proton-induced production of ^{26}Al from aluminum, manganese, iron and nickel.

E ± dE [MeV]	σ ± dσ [mb]	E [MeV]	σ ± dσ [mb]
$^{27}Al(p,pn)^{26}Al$		**$Fe(p,14pxn)^{26}Al$**	
66.7 ± 0.8	71.2 ± 5.3	189.	≤ 0.010
80.0 ± 0.3	70.8 ± 4.4	600.	0.543 ± 0.036
95.5 ± 0.2	54.4 ± 4.0	800.	0.904 ± 0.062
155.3 ± 1.1	29.4 ± 1.5	1200.	1.74 ± 0.09
200.0 ± 1.4	27.7 ± 1.5	2600.	2.22 ± 0.13
600.	22.6 ± 1.0		
800.	23.4 ± 1.5	**$Ni(p,16pxn)^{26}Al$**	
1200.	22.5 ± 1.6		
2600.	20.0 ± 1.4	148.	≤ 0.262
		600.	0.393 ± 0.072
$Mn(p,13p17n)^{26}Al$		800.	0.763 ± 0.059
		1200.	1.62 ± 0.10
171.	≤ 0.055	2600.	2.75 ± 0.24
600.	0.460 ± 0.091		
800.	0.864 ± 0.095		
1200.	1.61 ± 0.13		
2600.	1.99 ± 0.22		

1.3 Production of Stable Rare Gas Isotopes by Proton-Induced Spallation Between 800 and 2600 MeV

In extraterrestrial matter stable cosmogenic nuclides can be observed as positive isotope abundance anomalies of rare gases. They are of particular importance in cosmochemistry and -physics because they integrate the effects of irradiation of the entire history of a meteorite or a lunar sample, provided that gas loss due to catastrophic events can be excluded. Moreover, rare gas isotopic ratios and even abundances can be measured with outstanding accuracy, so that it is possible to detect even minute effects. Therefore, the demands for highly reliable cross sections are even more stringent than for radionuclides, if one tries to model cosmogenic rare gases. However, the

presently available data base is also still inadequate and many of the older data (see [1-5] for a compilation) do not have sufficient accuracy.

Here, we report results for the proton-induced production of stable He- and Ne-isotopes from magnesium, aluminum and silicon and of stable He-, Ne-, and Ar-isotopes from Ni for energies of 800 MeV, 1200 MeV and 2600 MeV (table 4). Cross sections for a proton-energy of 600 MeV, measured by our collaboration were already reported earlier [14]. There one may find also details about the mass spectrometric procedure. The errors given for the cross sections contain those of the mass spectrometric measurements as well as that of the flux determination. It has, however, to be remembered that no error was assigned to the monitor cross sections. The measurements of cross sections for the production of stable rare gas isotopes will be extended to further target elements and lower proton-energies in the near future.

The data of this work were measured for targets irradiated at LNS and LANL, as described in section 1.1. Cross sections for stable isotope production necessarily are cummulative data, i.e. they contain the contributions from the decay of radioactive precursors. This is not the case for ^{22}Ne and ^{3}He, for which usually independent ones are given, which do not contain the contributions of the decays of ^{22}Na and ^{3}H, respectively. Thus, the cross sections for the production of ^{22}Ne are corrected for the decay of the ^{22}Na. The correction was done exclusively by ^{22}Na cross sections measured in the same experiments.

For ^{3}He our new cross sections, which should be considered as independent ones, are systematically too high by up to 10 %, because we do not yet have adequate cross sections for the production of ^{3}H from Mg, Al, Si, and Ni which would allow to subtract the ^{3}He-amount originating from the decay of ^{3}H between end of irradiation and mass spectrometric measurements. An early measurement of the irradiated targets is not possible for reasons of radiation protection. The irradiations ended on July 22, 1988 (800 MeV), December 15, 1987 (1200 MeV) and March 15, 1988 (2600 MeV). The mass spectrometric measurements were performed between November 11 and 14, 1989. With these dates it will be possible to correct the ^{3}He cross sections as soon as ^{3}H cross sections are available.

Tab. 4: Cross sections for the production of stable rare gas isotopes from magnesium, aluminum, silicon, and nickel by high-energy protons.

Reaction	Cross sections [mb] at a proton-energy of 800 MeV	1200 MeV	2600 MeV
Mg(p,11pXn)^{3}He	44.5 ± 1.9	56.9 ± 2.3	61.9 ± 2.6
Mg(p,11pXn)^{4}He	370. ± 15.	414. ± 17.	389. ± 16.
Mg(p,3pXn)^{20}Ne	31.7 ± 1.9	33.7 ± 2.0	25.3 ± 1.6
Mg(p,3pXn)^{21}Ne	31.7 ± 1.3	30.7 ± 1.3	24.8 ± 1.1
Mg(p,3pXn)^{22}Ne	15.4 ± 1.6	15.6 ± 2.0	12.1 ± 1.5
Al(p,12p13n)^{3}He	45.4 ± 4.8	57.0 ± 2.4	62.6 ± 2.7
Al(p,12p12n)^{4}He	375. ± 16.	428. ± 18.	399. ± 17.
Al(p,4p4n)^{20}Ne	26.4 ± 1.6	25.7 ± 1.6	20.5 ± 1.3
Al(p,4p3n)^{21}Ne	27.3 ± 1.1	26.5 ± 1.1	21.2 ± 0.9
Al(p,4p2n)^{22}Ne	15.4 ± 0.8	14.7 ± 0.8	12.1 ± 0.7
Si(p,13pXn)^{3}He	56.8 ± 2.4	74.3 ± 3.0	77.1 ± 3.3
Si(p,13pXn)^{4}He	403. ± 17.	458. ± 19.	405. ± 17.
Si(p,5pXn)^{20}Ne	27.0 ± 1.6	26.0 ± 1.6	19.6 ± 1.2
Si(p,5pXn)^{21}Ne	24.5 ± 1.0	23.6 ± 1.0	17.8 ± 0.8
Si(p,5pXn)^{22}Ne	9.38 ± 1.05	9.07 ± 1.20	6.81 ± 0.88
Ni(p,27pXn)^{3}He	70.1 ± 2.9	92.7 ± 3.8	122. ± 5.

Tab. 4: (continued) Cross sections for the production of stable rare gas isotopes from magnesium, aluminum, silicon, and nickel by high-energy protons.

Reaction	Cross sections [mb] at a proton-energy of 800 MeV	1200 MeV	2600 MeV
Ni(p,27pXn)^{4}He	546. ± 23.	662. ± 27.	744. ± 31.
Ni(p,19pXn)^{20}Ne	1.28 ± 0.19	2.85 ± 0.43	5.17 ± 0.78
Ni(p,19pXn)^{21}Ne	1.46 ± 0.07	3.05 ± 0.16	5.53 ± 0.29
Ni(p,19pXn)^{22}Ne	0.821 ± 0.081	1.74 ± 0.16	3.13 ± 0.29
Ni(p,11pXn)^{36}Ar	2.14 ± 0.15	2.66 ± 0.19	2.21 ± 0.16
Ni(p,11pXn)^{38}Ar	12.8 ± 0.7	14.9 ± 0.8	12.5 ± 0.6

2. Excitation Functions of Proton-Induced Reactions up to 100 MeV

B. Dittrich[1], U. Herpers[1], R. Bodemann[2], R. Michel[2], H. Condé[3], B. Holmqvist[4], P. Malmborg[3]

The project, from which first results are reported here, is intended to measure integral excitation functions for the production of residual nuclides by proton-induced reactions up to 200 MeV. Such excitation functions are the basic data for an accurate modelling of the interactions of solar cosmic ray particles with terrestrial and extraterrestrial matter. They are essential for design and optimization of radionuclide production and - last not least - they are useful to test nuclear reaction theories.

The present work is mainly related to cosmochemical aspects and to tests of nuclear reaction theories in the transition zone between pre-equilibrium and spallation. The proton-irradiations were carried out at the cyclotron of the Svedberg Laboratory of the University Uppsala. Up to now, proton-energies up to 100 MeV are available at this accelerator. Experiments with higher energies are scheduled for 1990. Radioactive residual nuclides were determined by gamma-spectrometry and accelerator mass spectrometry, stable rare gas isotopes by conventional mass spectrometry.

The cross sections were determined using the stacked foil technique. Up to now, proton irradiations were performed which cover a total of 18 elements (C, N as Si_3N_4, O as SiO_2, Mg, Al, Si, Ti, V, Mn as Mn/Ni-alloy, Fe, Co, Ni, Cu, Zr, Nb, Rh, Ba as a Ba-containing glass, and Au). Beam monitoring was done by investigating the production of ^{22}Na from Al, for which evaluated cross sections exist [11]. Consistency between the evaluated excitation function of the monitoring reaction and the measured data (Fig. 2) could only be obtained, if a shift of the initial proton-energy to lower energies of 4 MeV was assumed. Exact measurements of the initial proton-energies using time-of-flight techniques and range measurements are presently performed by the accelerator staff, but not yet finished.

1 Abteilung Nuklearchemie, Universität zu Köln, F.R.G.
2 Zentraleinrichtung für Strahlenschutz, Universität Hannover, F.R.G.
3 The Svedberg Laboratory, University Uppsala, Sweden
4 The Studsvik Neutron Research Laboratory, University Uppsala, Sweden

It is a matter of course that there is faster progress for the gamma-spectrometric measurements than for the mass spectrometric ones. The latter can only be started after finishing the non-destructive measurements and after cooling down of the radioactivity. Therefore, presently most results are for gamma-emitting nuclides. The cross sections measured up to now describe more than 120 individual reactions. In figs. 3 and 4 some examples are given, describing the typical status of the data. There are reactions as $Fe(p,xn)^{58}Co$ (Fig. 3), where our new measurements fill gaps in former measurements, others, as $Si(p,3p)^{28}Mg$ (Fig. 4), for which no data existed before, and a third type, where our measurements allow to clear up existing discrepancies, as for $O(p,5pxn)^{7}Be$ (Fig. 4). The quality of the new data is thoroughly checked by remeasuring a number of reactions which have been investigated earlier by our group [6, 7]. Here, good agreement could be obtained. The new data will be applied to model calculations of the production of solar cosmic ray produced nuclides in lunar surface materials and will be discussed in the context of theories of preequilibrium and spallation reactions.

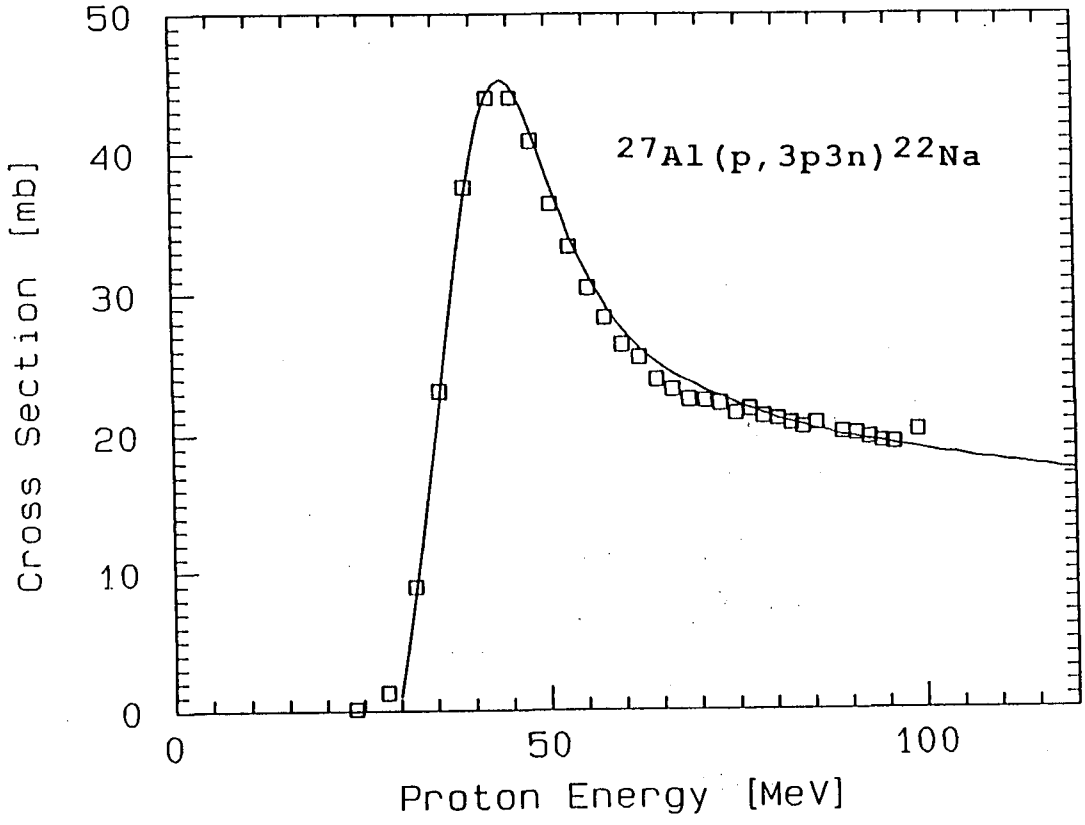

Fig. 2: Measured cross sections for the reaction $^{27}Al(p,3p3n)^{22}Na$ (open squares) in comparison with the evaluated excitation function (full line). The experimental errors of this work are smaller then the symbols used.

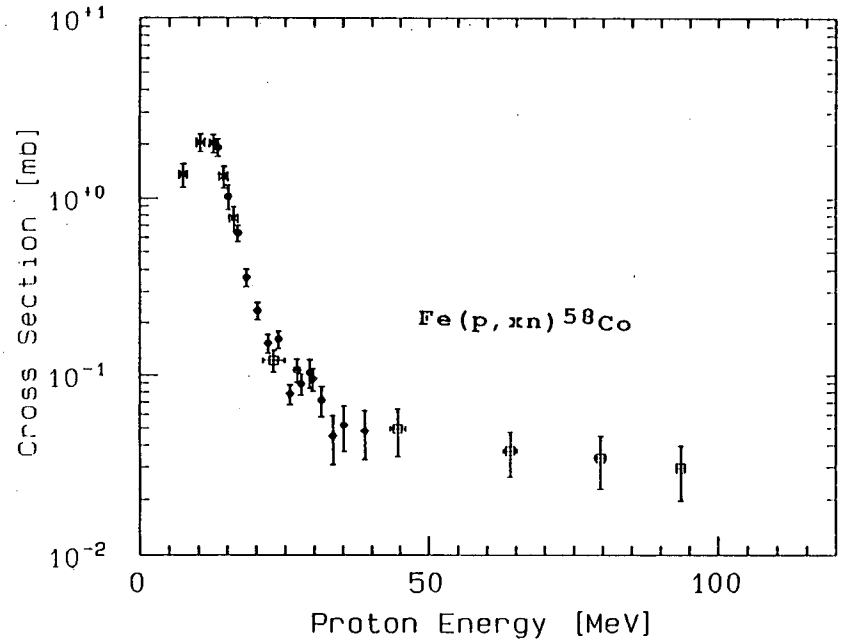

Fig. 3: Excitation function for the reaction Fe(p,xn)^{58}Co, consisting of data from this work (open squares with error bars) and of earlier work from our group. The new data complete the excitation function at higher energies and give a smooth transition to the earlier data.

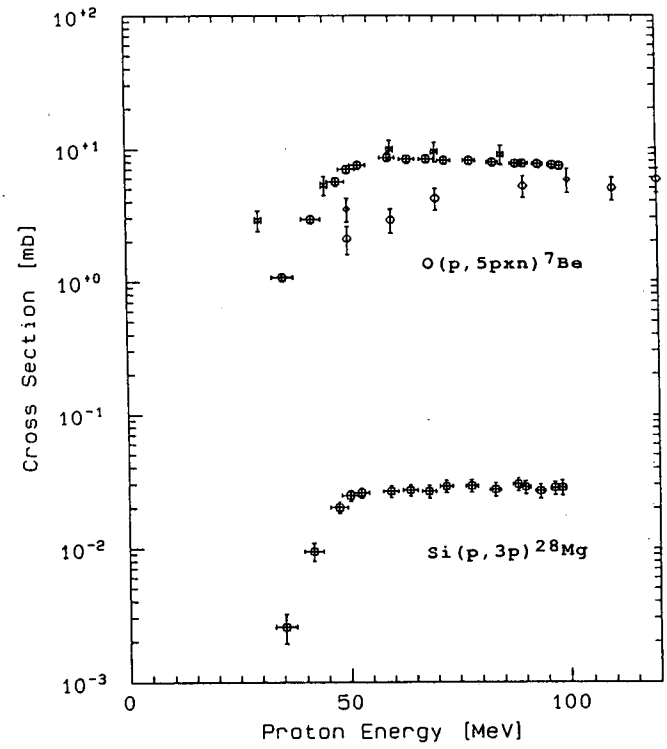

Fig. 4: Excitation functions for the reactions Si(p,3p)^{28}Mg and O(p,5pxn)^{7}Be measured in this work. The data from this work are plotted as open squares with error bars. For the production of ^{7}Be from O, the new data clear up a discrepancy between earlier data from different authors (⬭, ◇, ⋈ denote data from refs. [23-25], respectively.

References

[1] F.K. McGowan, W.T. Milner, Atomic Data Nucl. Data Tables (1976) 18, 1.

[2] T.W. Burrows, P. Dempsey, P., BNL-NCS-50640, 4th Edition (1980).

[3] T.W. Burrows, G. Wyant, BNL-NCS-50640, 4th Edition, Suppl. 1 (1981).

[4] N.E. Holden, T.W. Burrows, BNL-NCS-50640, 4th Edition, Suppl. 2 (1982).

[5] N.E. Holden, S. Ramavataram, C.L. Dunford, BNL-NCS-51771 (1985).

[6] R. Michel, F. Peiffer, R. Stueck, Nucl. Phys. A 441 (1985) 617.

[7] R. Michel, R. Stück, J. Geophys. Res. (Suppl.) 89 B (1984) 673.

[8] R. Michel, B. Dittrich, U. Herpers, T.Schiffmann, P. Cloth, P. Dragovitsch, D. Filges, The Analyst 114 (1989) 287.

[9] B. Dittrich, U. Herpers, M. Lüpke, R. Michel, H.J. Hofmann, W. Wölfli, Determination of Cross Sections for the Production of 7Be, 10Be and 22Na by High Energy Protons, Radiochim. Acta, (1990) in press.

[10] B. Dittrich, U. Herpers, H.J. Hofmann, W. Wölfli, M. Lüpke, R. Michel, P. Dragovitsch, D. Filges, AMS measurements of thin-target cross sections for the production of ^{10}Be and ^{26}Al by high-energy protons, submitted to Nucl. Instr. Meth. Phys. Res. B (1989).

[11] J. Tobailem, C.H. de Lassus St. Genies, Additif No. 2 a la CEA-N-1466(1) (1975), CEA-N-1466(5) (1981).

[12] W. Seelmann-Eggebert, G. Pfennig, H. Muenzel, H. Kleve-Nebenius, Chart of the Nuclides, 5th Edition, Kommunalschriften-Verlag Jehle, Muenchen (1981).

[13] U. Reuss, W. Westmeier, Atomic Data Nucl. Data Tables 29 (1983)1 and ibid. 193.

[14] R. Michel, F. Peiffer, S. Theis, F. Begemann, H. Weber, P. Signer, R. Wieler, P. Cloth, P. Dragovitsch, D. Filges, P. Englert, Nucl. Instr. Meth. Phys. Res. B42 (1989) 76 - 100.

[15] B. Dittrich, U. Herpers, M. Lüpke, R. Michel, in: Progress Report on Nuclear Data Research in the Federal Republic of Germany for the Period April, 1st, 1988 to March, 31th, 1989, NEANDC(E)-292 U Vol. V INDC(Ger)-34/LN+Special (1989) 31.

[16] R. Silberberg, C.H. Tsao, Astrophys. J. Suppl. 25 (1973) 315.

[17] P. Cloth, D. Filges, R.D. Neef, G. Sterzenbach, C. Reul, T.W. Armstrong, B.L. Colborn, Juel-2203 (1988).

[18] M. Blann, Phys. Rev. Lett. 27 (1971) 337.

[19] M. Blann, priv. comm. (1987).

[20] R. Michel, P. Dragovitsch, P. Englert, F. Peiffer, R. Stück, S. Theis, F. Begemann, H. Weber, P.Signer, R. Wieler, D. Filges, P. Cloth, Nucl. Instr. Meth. Phys. Res. B16 (1985) 61.

[21] S. Vogt, U. Herpers, Fresenius Z. Anal. Chem. 331 (1988) 186.

[22] B. Dittrich, Thesis, Univ. zu Köln (1990).

[23] G. Albouy, J.P. Cohen, M. Gusakov, N. Poffe, H. Sergolle, L. Valentin, Phys. Lett. 2 (1962) 306.

[24] R. Bimbot, H. Gauvin, Compt. Rend. Ser. B 273 (1971) 1054.?

[25] M.S. Lafleur, N.T. Porile, L. Yaffe, Can. J. Chem. 44 (1966) 2749.

INSTITUT FÜR KERNCHEMIE
UNIVERSITÄT MAINZ

Mass yields in the chains with A = 72 - 87 in the fission of ^{249}Cf by thermal neutrons

R. Hentzschel, H. O. Denschlag, H. R. Faust[1], J. E. Gindler[2], B. Wilkins[2]

Mass yields in the fission of ^{249}Cf induced by thermal neutrons have been measured in the chains with the mass numbers A = 72 to 87 using the mass separator LOHENGRIN at the Institut Laue-Langevin in Grenoble. The result of a first evaluation is shown in Fig. 1 together with values obtained by Djebara et al. [1]. The experimental values may be compared there with the yields as predicted in the US ENDF-V file [2]. It appears that the experimental yields of the very light fission fragments are considerably higher than predicted. The discrepancy amounts to nearly a factor of 100 for mass 72. The exact experimental yield values will be reported in the next report of this series.

References

[1] M. Djebara, M. Asghar, J. P. Bocquet, R. Brissot, J. Crançon, Ch. Ristori, E. Aker, D. Engelhardt, J. Gindler, B. D. Wilkins, U. Quade, K. Rudolph: Mass and Nuclear Charge Yields for ^{249}Cf(n_{th},f) at Different Fission-Product Kinetic Energies; Nucl. Phys. A496, 346-366 (1989).

[2] B. F. Rider, Compilation of Fission Product Yields, Vallecitos Nuclear Center 1981, Report NEDO-12154-3(C), ENDF-322, October 31, 1981.

---

[1] Institut Laue-Langevin, Grenoble, France
[2] Argonne National Laboratory, Argonne, Illinois, USA

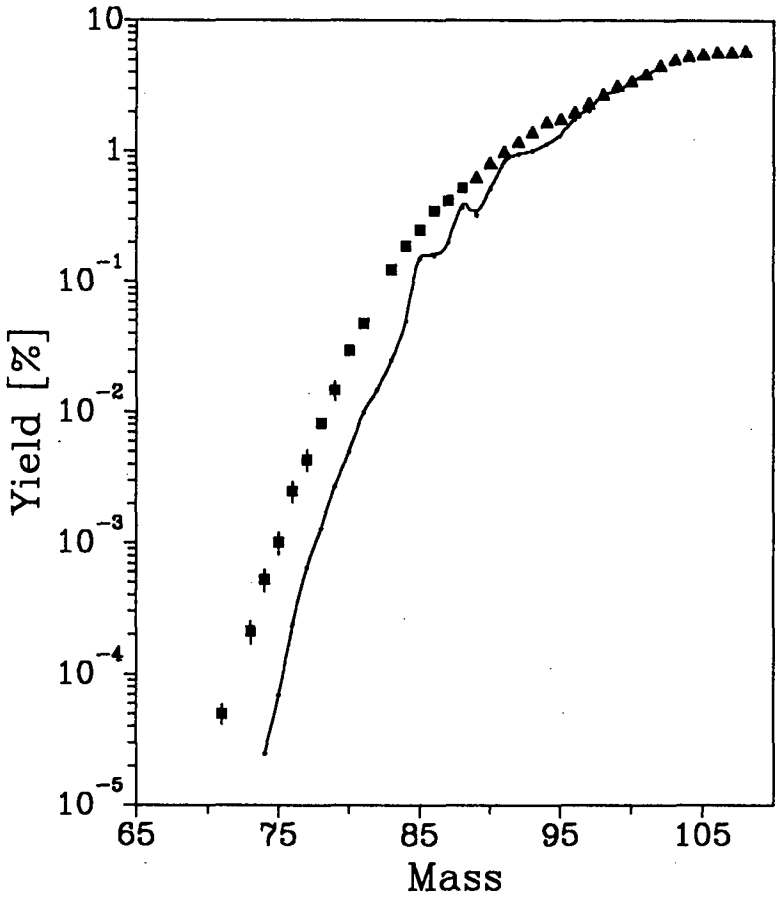

Fig. 1: Experimental chain yields in the fission of ^{249}Cf by thermal neutrons (Triangles from [1] and squares [this work]) and predicted values (drawn out line) [2].

FRM-REAKTORSTATION GARCHING, FACHBEREICH PHYSIK
TECHNISCHE UNIVERSITÄT MÜNCHEN

Coherent Neutron Scattering Lengths and Total Cross Sections

1. Neutron Scattering Lengths of Molten Metals Determined by Gravity Refractometry
G. Reiner, W. Waschkowski and L. Koester

Very accurate values of the coherent neutron scattering lengths of the heavy elements Bi and Pb are important quantities for the investigation of the electric interactions of neutrons with atoms.

We performed, therefore, a series of experiments to determine accurate scattering lengths by means of neutron gravity refractometry on liquid mirrors of molten metals. The possible perturbations of the necessary reflection measurements have been discussed in datail.

After taking into account the uncertainties and corrections associated with observable pertubations we obtained the following values for bound atoms:
b(Bi)=8.532±0.002 fm, b(Pb)=9.405±0.003 fm, b(Tl)=8.776±0.005 fm, b(Sn)=6.225±002 fm and b(Ga)=7.288±0.002 fm.

These data are corrected for the local field effect occuring in the reflection on liquids. The recently reported results for the neutron's electric polarizability and the neutron-electron scattering length are supported by the Bi- and Pb scattering length of this work.
Submitted to Z. Phys. A- Atomic Nuclei
Accepted

2. Cross Sections for Neutrons of 1970 eV and Contributions to Fundamental Neutron Interactions
L. Köster, W. Waschkowski and J. Meier

Neutrons of energies within a 50 eV interval at 1970 eV have been selected from reactor neutrons by means of neutron resonance scattering on a target of ^{63}Cu and subsequent scattering by the 1970 eV resonance of a ^{80}Se target. The insertion of stationary filters of Sc, Co and B and the technique of difference measurements with a resonance filter resulted in a high selectivity, which allowed the determination of cross sections for quasimonoenergetic neutrons.
Values of total cross sections at 1970 eV are given for the elements H,C,O,F,Na,Mg,Al,Si,P,Cl,K,Ca,Sc,Ti,V,Mn,Co,Ni,Cu,Ga,Pb and Bi.

Substance	σ_{tot} (1970 eV) [b]		Substance	σ_{tot} (1970 eV) [b]	
H	20.13	(3)	Ca	2.43	(5)
C	4.744	(5)	Sc	0.27	(2)
O	3.77	(3)	Ti	5.17	(2)
F	3.59	(1)	V	7.61	(2)
Na	12.77	(4)	Mn	125	(2)
Mg	3.35	(5)	Co	1.35	(2)
Al	1.350	(7)	Ni	15.04	(3)
Si	2.019	(5)	Cu	29	(1)
P	3.23	(2)	Ga	8.41	(4)
Cl	1.60	(3)	Pb	11.198	(3)
K	1.58	(4)	Bi	8.292	(3)

The precision cross sections of Pb and H are of particular interest for the investigation of fundamental neutron interactions.
In combination with cross sections at lower energies, the cross section σ (Pb)= 11.198 ± 0.003 b has been used to derive a value of α_n= (0.7±1) 10^{-3} fm ^{3} for the electric polarizability of the neutron, by which the recently published values are confirmed.
The neutron-proton cross section σ (^{1}H) = 20.13 ± 0.03 b and data at 143 keV, <1.3> MeV, <2.1> MeV and values for the literature allowed to estabish a refined set of the neutron-proton scattering parameters for the shape-independent effective-range approximation of the neutron-proton interaction.

Submitted to Z. Phys. A. - Atomic Nuclei

INSTITUT FÜR STRAHLENPHYSIK
UNIVERSITÄT STUTTGART

1. Nuclear Astrophysics

A. Denker, H. Drotleff, J.W. Hammer, H. Knee, A. Köhler, S. Küchler, C. Rolfs, D. Streit

Neutron-producing α, n-reactions: $^{22}Ne(\alpha,n)^{25}Mg$

In collaboration with H.P. Trautvetter, Münster and K.L. Kratz, Mainz.

The $^{22}Ne(\alpha,n)^{25}Mg$-reaction is supposed as one of the relevant neutron-producing reactions for the astrophysical s-process. However recent investigations [1] showed, that the reaction rate of the $^{22}Ne(\alpha,\gamma)^{26}Mg$-reaction is significantly higher than assumed previously and therefore the ratio of the rates for $^{22}Ne(\alpha,n)^{25}Mg$ and $^{22}Ne(\alpha,\gamma)^{26}Mg$ will be smaller by at least a factor of 60 near $T_9 = 0.65$ unless new low lying resonances in the (α,n)-branch will be found. The neutron data suffer from some experimental problems compared with the gamma measurements, because neutron detectors with high efficiency deliver none or only poor energetic information and one has to consider disturbing background reactions with neutrons in the same energy range. Therefore several experimental attempts have been made to overcome this background problem and to obtain cross section data in the neutron channel with more significance. First, one was using inverse kinematics in this reaction, which means neon-22 as projectile and helium-4 as target to avoid contributions of the comparable strong $^{13}C(\alpha,n)^{16}O$-reaction. With the currents available at present (0.5 μA) measurements in the energy range 1000-1200 keV (cm) could be performed and it could be demonstrated, that with this kind of measurement the problem of background reactions is solved. But further experiments at cm-energies below 1000 keV are only possible if $^{22}Ne^{2+}$-currents are available in the range 50-100 μA . With inverse kinematics the neutron energies are raised in the laboratory system, which is helpful for neutron-detection. Second, an experiment with regular kinematics has been performed with improving some essential experimental conditions:

- improvement of the beam emittance, transmission of the beam through the gas target for energies >1 MeV is nearly 100 %.
- very clean conditions at the apertures of the gas target, where the beam could hit solid material; efficient cleaning of the gas.
- nearly 4π-detection of the neutrons by applying neutron moderation in paraffin and detection of the thermalized neutrons in ^3He-proportional counters: the reaction chamber was a stainless steel tube of 1m length covered inside with tantalum.
- supervision of the background contribution by measuring background in separate runs for every beam setting.

The excitation function of $^{22}Ne(\alpha,n)^{25}Mg$ has been measured with a target pressure of 0.3 mbar (Fig. 1) and 0.1 mbar (Fig. 2), the latter giving more details at small resonances. There is good agreement with previous measurements of our group using NE 213-detectors. There is also good agreement concerning the energy and the width of the resonances with the measurements of Wolke et al. where the excitation function of the n_1- and the n_2-group had been determined by gamma

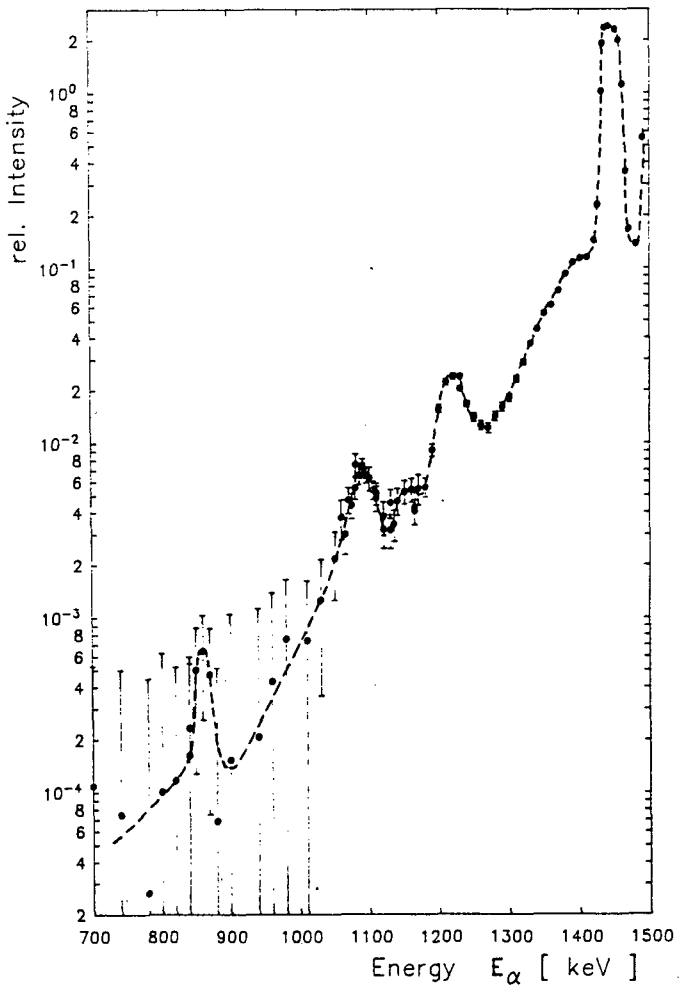

Fig.1 Excitation function of $^{22}Ne(\alpha,n)^{25}Mg$ using enriched neon-22 as targetgas at a pressure of 0.3 mbar, the energy is given in the laboratory system, the neutron yield is in arbitrary units and the line is used as guide for the eye. The beam current was monitored by counting elastic scattered events in a particle detector located at 90° to the beam axis.

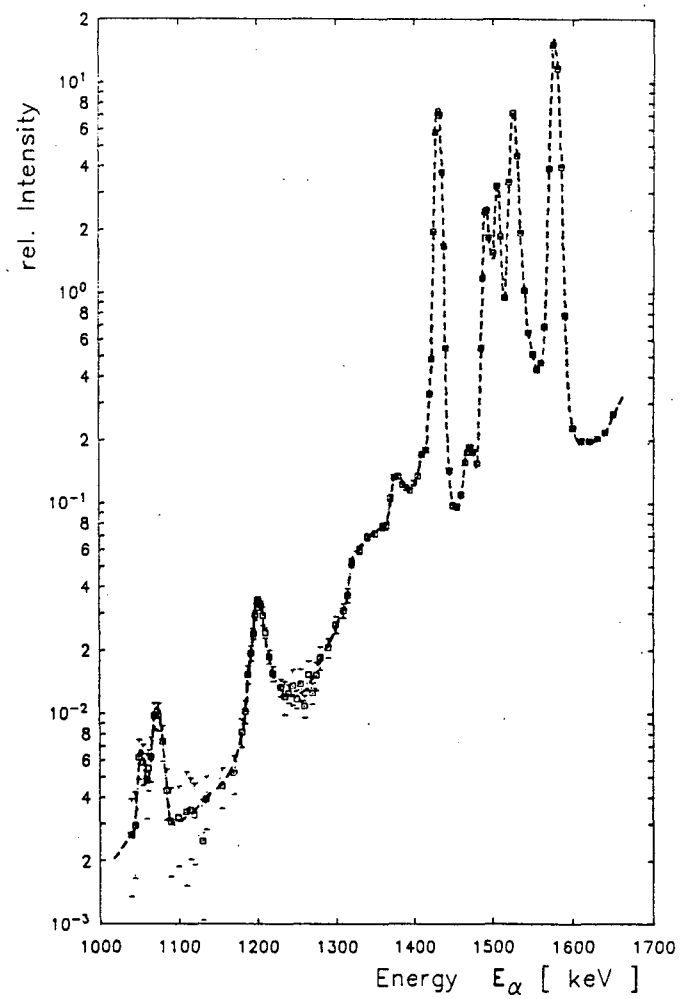

Fig.2 Excitation function of $^{22}Ne(\alpha,n)^{25}Mg$ measured at a target pressure of 0.1 mbar, to obtain the fine structure of the curve, which is only a guide for the eye.

spectroscopy.

The resonances at about 1200, 1070, 1050 and 840 keV differ from previous measurements also given in the paper of Wolke [1]: only one resonance has been determined at 1200 keV, but two at 1070 and 1050 keV. The resonance at 840 keV has been found to be weaker than in the paper of Wolke et al. [1] as can be seen in Fig.1. The energy region below 800 keV will be subject of further investigations, needing a longer beam time.

The $^{13}C(\alpha,n)^{16}O$ reaction

The $^{13}C(\alpha,n)^{16}O$-reaction is also considered as a possible neutron source in stars. The experimental data of this reaction have been reanalyzed, especially the unfolding of the proton recoil spectra was improved. The total cross section was determined by using measured angular distributions of the neutrons. With these revised data the astrophysical S-factor was calculated and the result is shown in Fig. 3. The S-factor is increasing considerably at energies below 400 keV (cm) as it was predicted by the calculations of Descouvemont [2].

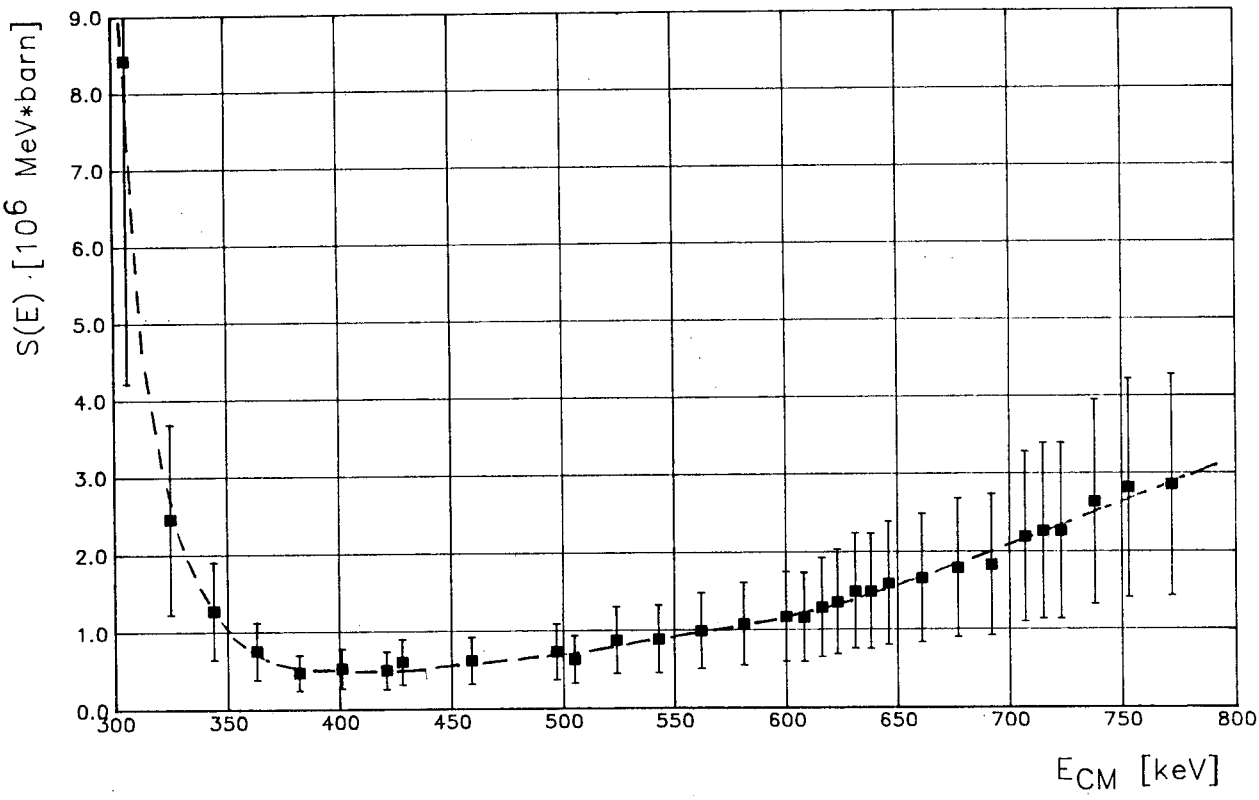

Fig.3 Astrophysical S-factor of the reaction $^{13}C(\alpha,n)^{16}O$ measured using proton recoil spectrometers (NE 213). The curve is based on the determination of the total cross section obtained as well from measurements of angular distributions as from runs in close geometry.

The reactions $^{25}Mg(\alpha,n)^{28}Si$ and $^{26}Mg(\alpha,n)^{29}Si$

The reactions $^{25}Mg(\alpha,n)^{28}Si$ and $^{26}Mg(\alpha,n)^{29}Si$ have been studied using enriched targets of metallic magnesium, which were reduced from the oxide and were evaporated on a copper backing. Excitation functions have been obtained for both reactions for targets of different thickness down to the limit of of neutron detection, which means, that the cross section could be determined more sensitively by about two orders of magnitude than in former experiments. Fig. 4 is showing the result for the case of the $^{26}Mg(\alpha,n)^{29}Si$-reaction, exhibiting many resonances not detected in previous experiments in the neutron channel.

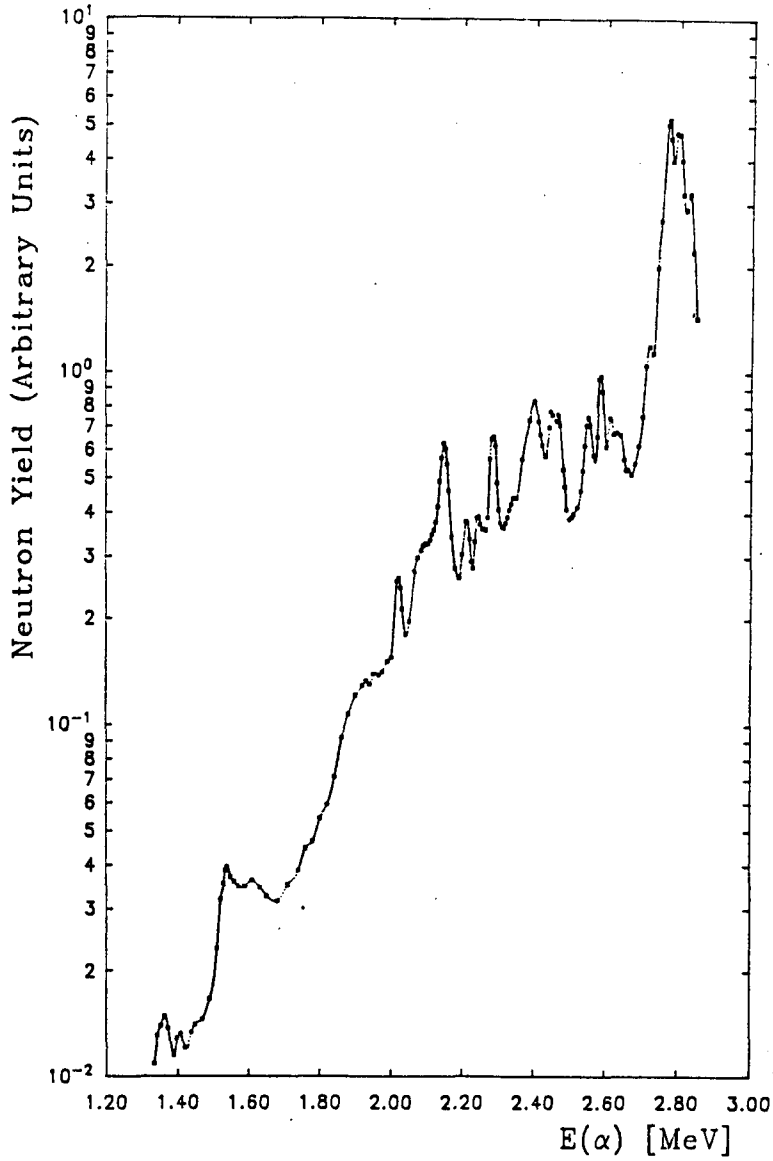

Fig.4 Excitation function of the $^{26}Mg(\alpha, n)^{29}Si$-reaction measured by NE 213 detectors in close geometry. The target was evaporated in metallic composition on a copper backing.

The fusion reaction ^{12}C - ^{12}C.

The fusion reaction ^{12}C - ^{12}C is the key reaction in massive stars after the helium burning stage. Because of the exceptional behaviour of the cross section exhibiting many resonances the extrapolation of the S-factor towards lower energies requires still more experimental data. Previous measurements using solid state targets came to a limit of sensitivity at a cm-energy of about 2.5-3 MeV because of problems with some unavoidable hydrogen content of the targets and the stability of the targets itself [3], [4]. Therefore an experiment has been performed using the gastarget facility RHINOCEROS in the supersonic jet configuration and using a carbon beam of the Bochum Dynamitron tandem accelerator in the energy range E_{cm} = 2.75-5.75 MeV. Very clean CO_2 has been used as target gas with a target density of about 5 $\mu g/cm^2$. Protons, α-particles and gammas were detected in one experimental setup. It came out as a result, that there is no problem with hydrogen contamination and that there was good agreement with previous measurements. The investigation will be prosecuted after improving the efficiency of the detectors and the density of the target.

References

[1] K. Wolke et. al. : Z.Phys. **A 334** (1989) 491

[2] Descouvemont, P. : Phys.Rev. **C 36** (1987) 2206

[3] K.U. Kettner et. al. : Z.Phys. **A 298** (1980) 65

[4] H.W. Becker et al. : Z.Phys. **A 303** (1981) 305

2. Polarized Neutron Scattering Data for ^{55}Mn, ^{nat}Fe, ^{59}Co, and ^{nat}Ni

W. Grum, J.W. Hammer, K.-W. Hoffmann and G. Schreder

Polarized neutron scattering data for nuclei in the Fe–region were measured at the Stuttgart SCORPION facility. The differential cross sections and analyzing powers were obtained at 7.68 MeV for ^{55}Mn and ^{59}Co, and at 7.75 MeV for ^{nat}Fe and ^{nat}Ni. In addition to ^{9}Be$(\alpha,\vec{n})$ usually applied as n-source a run with the source ^{13}C$(\alpha,\vec{n})$ was performed for ^{nat}Ni at 5.33 MeV. At the corresponding α-energy of 3.3 MeV the n-polarization reaches its maximum of only –17% at $\phi = 22°$, thus leading to the poorer statistics of Fig.2. A more detailed description of ^{13}C$(\alpha,\vec{n})$ can be found in Ref.1. So far only the elastic data for ^{nat}Ni have been corrected for multiple scattering effects (Fig.1), Figs.2–5 show the results of the unfolded NE213–recoil-spectra. The cross sections are normalized to hydrogen in a polyethylene-sample. A detailed description of the SCORPION setup and the various methods of data evaluation can be found in Ref. 2. The curves are Legendre polynomial fits to the data. The optical model analysis will be carried out after the completion of the multiple scattering corrections.

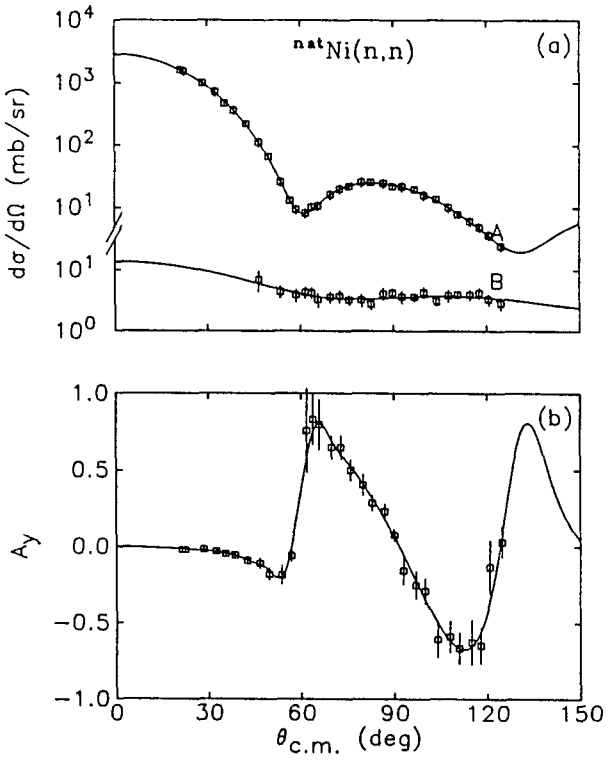

FIG. 1. Angular distributions of scattering data for ^{nat}Ni at E_n =7.75 MeV. (a) Corrected elastic(A) and inelastic(B) differential cross section, (b) analyzing power of elastic scattering.

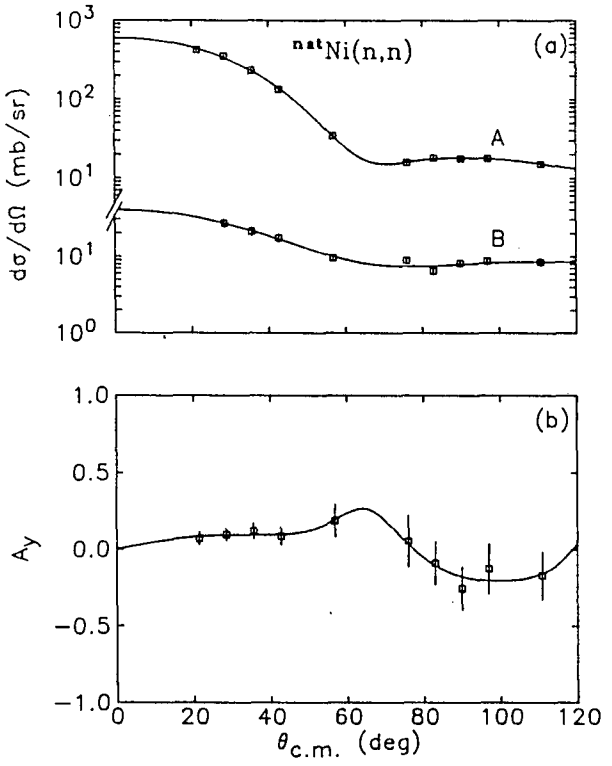

FIG. 2. Angular distributions of scattering data for ^{nat}Ni at E_n =5.33 MeV. (a) Elastic(A) and inelastic(B) differential cross section, (b) analyzing power of elastic scattering.

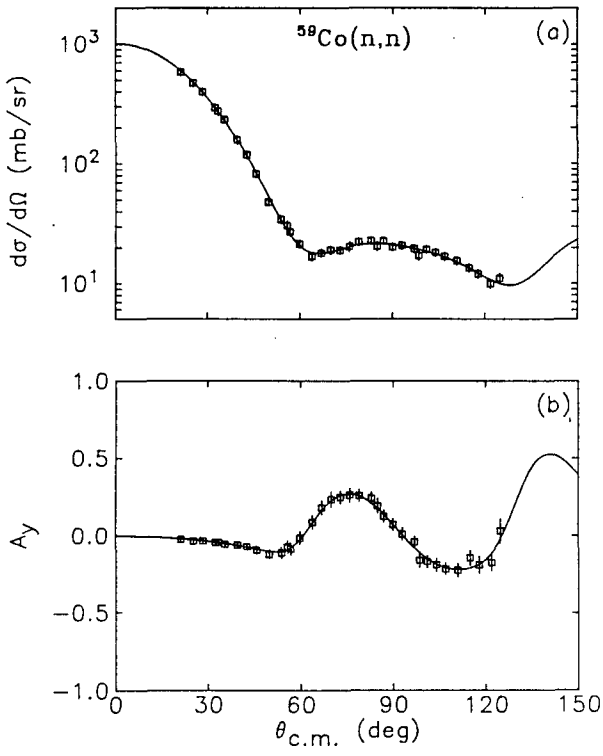

FIG. 3. Angular distributions of elastic scattering for ^{59}Co at E_n =7.68 MeV. (a) Differential cross section and (b) analyzing power.

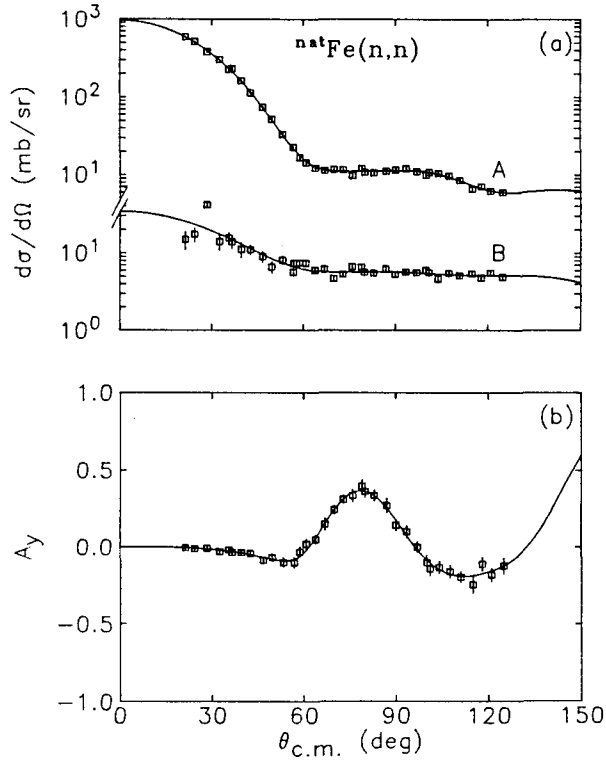

FIG. 4. Angular distributions of scattering data for ^{nat}Fe at E_n =7.75 MeV. (a) Elastic(A) and inelastic(B) differential cross section, (b) analyzing power of elastic scattering.

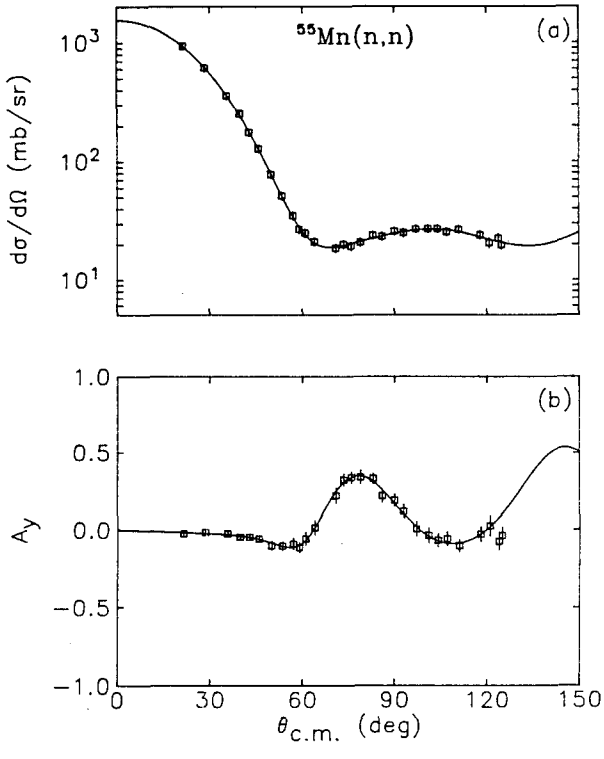

FIG. 5. Angular distributions of elastic scattering for ^{55}Mn at E_n =7.68 MeV. (a) Differential cross section and (b) analyzing power.

[1] W. Weiss, W. Grum, J.W. Hammer, and G. Schreder, accepted for publication in NIM **A** (1990).

[2] J.W. Hammer, G. Bulski, W. Grum, W. Kratschmer, H. Postner, and G. Schleußner, NIM **A244**, 455 (1986).

PHYSIKALISCH TECHNISCHE BUNDESANSTALT
BRAUNSCHWEIG

Neutron Cross Sections

1. Scattering Cross Sections of Carbon Between 13.4 and 15.8 MeV

G. Börker, W. Mannhart, B.R.L. Siebert

The cross sections of $^{12}C(n,n)^{12}C$ and $^{12}C(n,n')^{12}C^*$ (4.44 MeV) were determined at neutron energies of 13.33, 14.06, 14.53 and 15.82 MeV with a multi-angle neutron time-of-flight spectrometer. The data were normalized in relation to the n-p cross section by using an additional scattering sample of polyethylene. The n-p scattering data were carefully inspected to detect possible discrepancies due to incorrect neutron detector efficiencies or to incomplete corrections for multiple scattering processes. No such effects have been identified within a 2 % overall uncertainty .

For each neutron energy, the differential cross section was measured at 35 to 40 different angles between 12.5 and 160 degrees. The differential data on the elastic scattering are plotted in Fig. 1 and compared with ENDF/B-V. Whereas these differential data show large deviations from ENDF/B-V, the integral elastic cross sections of this experiment agree to within 5 % with the data of ENDF/B-V.

A remarkable agreement between the present data at 14.06 MeV and the recent evaluation of Hansen [1] performed at 14.1 MeV has been found for both the elastic and the inelastic cross section (see Fig. 2).

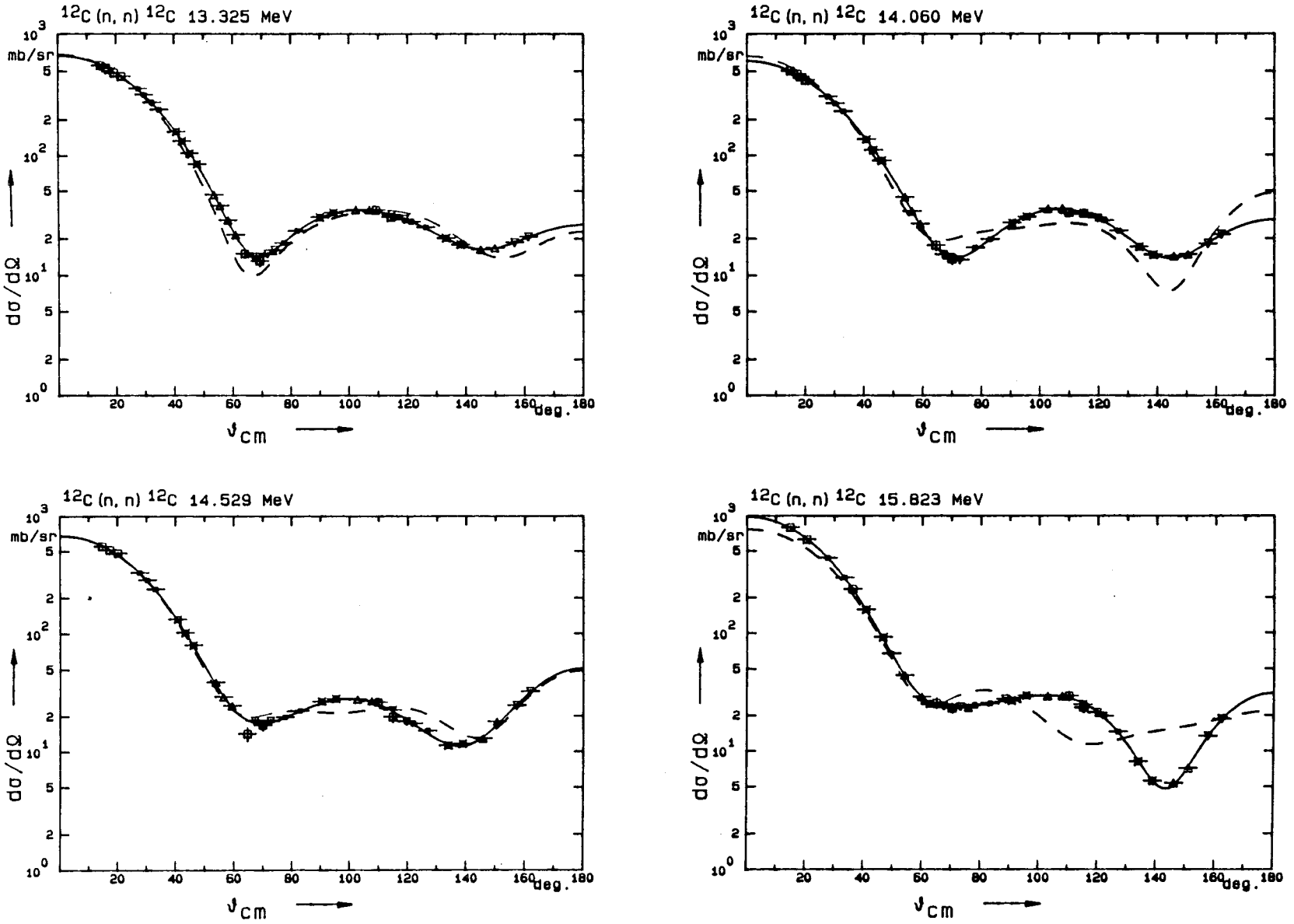

Fig. 1 Differential cross sections of elastic scattering on ^{12}C. The present data (symbols) are shown with a Legendre polynomial fit (solid line) and compared with ENDF/B-V (broken line).

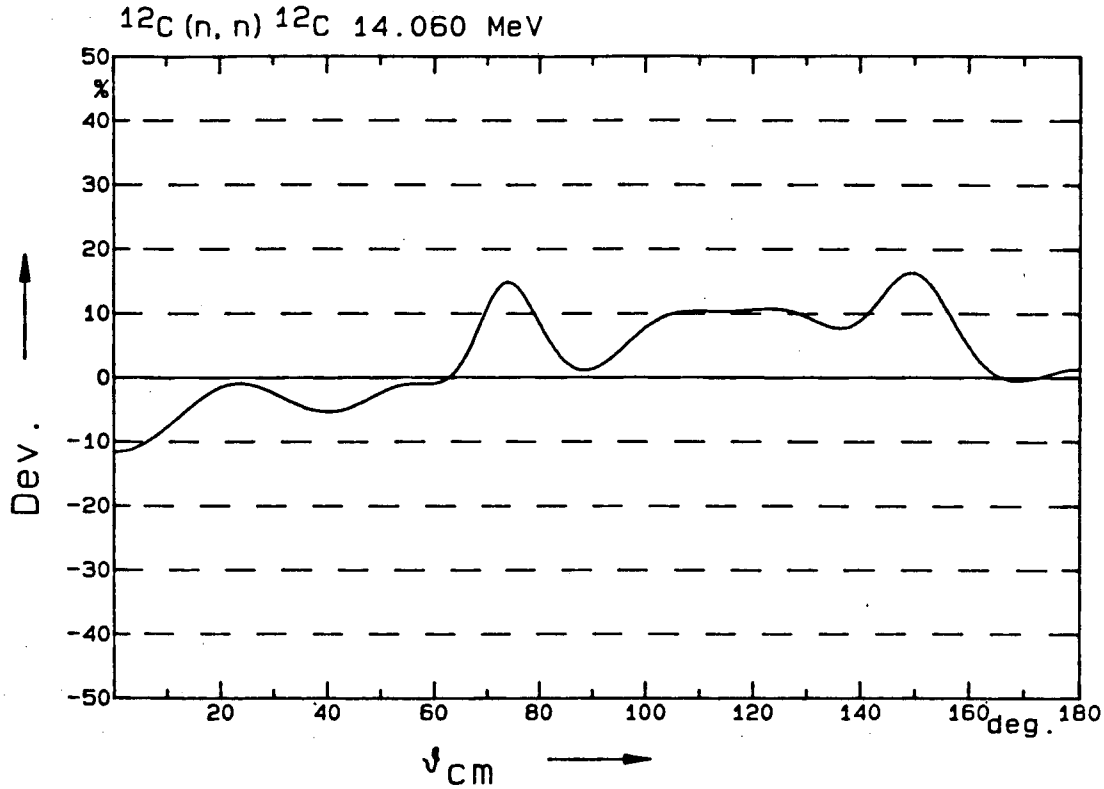

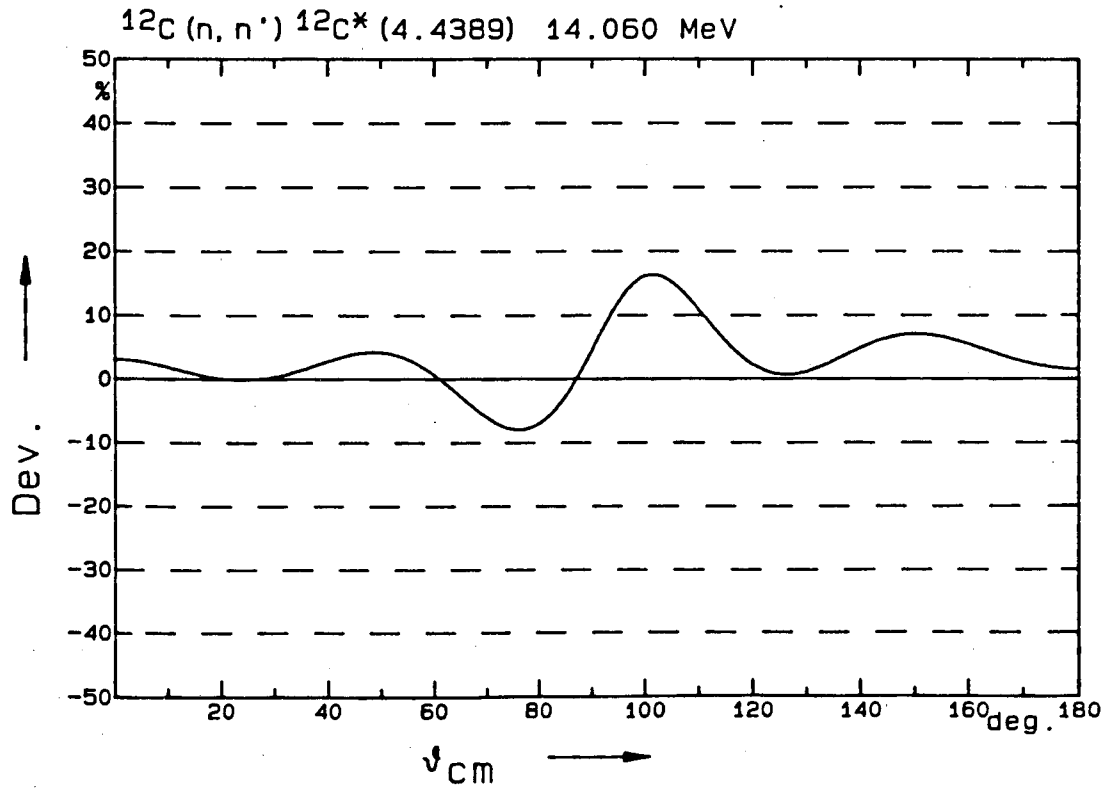

Fig. 2 Relative deviations of the present data (14.06 MeV) from the evaluation of Hansen [1] for elastic (upper part of the figure) and inelastic (lower part) scattering.

2. Measurement of the $^{47}Ti(n,p)^{47}Sc$ Reaction Cross Section

W. Mannhart, D.L. Smith*, J.W. Meadows*

In the neutron energy range between 1.2 and 8 MeV, the cross section of the reaction $^{47}Ti(n,p)$ was measured relative to the fission cross sections of $^{235}U(n,f)$ or $^{238}U(n,f)$. In parallel, the integral response of this reaction in a Cf-252 and a U-235 neutron spectrum was experimentally determined. All experiments were related to a common radioactivity counting detector. Special attention was paid to a precise calibration of the Ge(Li) detector at the low photon energy of 159.4 keV of ^{47}Sc.

The first results have been published elsewhere [2] and the final numerical data with a complete uncertainty description were recently released [3]. These data and their covariance matrix have been transferred to the NEA Data Bank for inclusion in the EXFOR file.

The results of this experiment gave cross section values which are substantially lower than those quoted by ENDF/B-V and removed a persistent discrepancy between integral and differential data on this reaction. While the $^{47}Ti(n,p)$ cross section between threshold and 8 MeV now seems to be well established, questions remain open regarding the absolute scaling of this cross section between 8 and 20 MeV which are exacerbated by the competitive $^{48}Ti(n,np)^{47}Sc$ reaction and by contradictory data in the literature.

3. Elastic and Inelastic Scattering Cross Section of Oxygen between 6 and 15 MeV

G. Börker, R. Böttger, H.J. Brede, H. Klein, W. Mannhart, B.R.L. Siebert

A complete documentation of the numerical data on this experiment [4] has been published as a laboratory report [5]. The data were also transferred to the NEA Data Bank (Paris) for future inclusion in the EXFOR data file.

*Argonne National Laboratory, Argonne, Ill. (USA)

The report contains the measured angular distributions of $^{16}O(n,n)^{16}O$ and $^{16}O(n,n')^{16}O^*$ (6.1 MeV) determined at 6.37, 7.51, 7.93, 9.01, 10.13, 10.16, 11.35, 12.49, 13.61 and 14.89 MeV neutron energy, together with the angle-integrated cross sections and the Legendre polynomial coefficients obtained from least-squares fits to the data. The corresponding uncertainties are quoted in the form of covariance matrices.

Besides these data, 10.16 MeV data were also determined for $^{9}Be(n,n)^{9}Be$, $^{9}Be(n,n')^{9}Be^*$ (2.43 MeV), $^{27}Al(n,n)^{27}Al$, $^{27}Al(n,n')^{27}Al^*$ (0.84 + 1.01 MeV), $^{28}Si(n,n)^{28}Si$, $^{28}Si(n,n')^{28}Si^*$ (1.78 MeV) and $^{28}Si(n,n')^{28}Si^*$ (4.62 MeV) with scattering samples of Be, BeO, Al, Al_2O_3, Si and SiO_2 instead of the H_2O samples finally used.

References

[1] L.F. Hansen, Report UCRL-95890 (December 1986)

[2] W. Mannhart, D.L. Smith, J.W. Meadows:
in "Nuclear Data for Basic and Applied Science",
(P.G. Young et al., Eds.), Gordon and Breach Science Publishers,
New York (1986) Vol. 1 pp 577

[3] W. Mannhart, D.L. Smith, J.W. Meadows:
Proc. of a Specialists' Meeting on Neutron Activation Cross Sections for Fission and Fusion Energy Applications, NEANDC-259 'U', OECD, Paris (1990) 121

[4] G. Börker, R. Böttger, H.J. Brede, H. Klein, W. Mannhart, B.R.L. Siebert:
in "Nuclear Data for Science and Technology", (S. Igarasi, Ed.),
Saikon Publ. Comp., Tokyo (1988) 193

[5] G. Börker, R. Böttger, H.J. Brede, H. Klein, W. Mannhart, B.R.L. Siebert:
Report PTB-N-1 (May 1989)

FACHINFORMATIONSZENTRUM KARLSRUHE

Status Report

H. Behrens, H.-W. Müller

1. Evaluated Nuclear Structure and Decay Data (ENSDF)

Nuclear Structure and Decay Data are evaluated by the International Network of Nuclear Structure and Decay Data Evaluators and published as the well-known Nuclear Data Sheets or in the Nuclear Physics journal. In addition, data are stored in the Evaluated Nuclear Structure Data File (ENSDF) from where they may be retrieved with respect to desired selection criteria. The Fachinformationszentrum Karlsruhe as a member of this network was responsible for the evaluation of the atomic mass range A = 81 to 100. From 1977 to 1989 the Fachinformationszentrum evaluated 23 mass chains in this range (5 mass chains have been re-evaluated after several years for actualization).

In 1989, the Fachinformationszentrum announced that it will discontinue the active evaluation of Nuclear Structure and Decay data.

From April 1, 1989 to March 21, 1990, the Fachinformationszentrum evaluated the four mass chains A = 85, 87, 89, and 91. The present status of these mass chains is as follows:

A = 89	published [1]
A = 85, 87	in review
A = 91	post review

Though the active evaluation has been stopped, the Fachinformationszentrum continues to distribute Nuclear Structure and Decay Data. However, online access is no longer possible, but data may be obtained from FIZ on request on magnetic tape or printout. The ENSDF file is updated twice a year. The present contents are as follows:

10,718 Datasets (each representing a special type of experiment or ADOPTED LEVELS, GAMMAS properties)

This information is stored on
921,192 Records (each of 80 byte length)

The MEDLIST data, which represent the radioactivity data of the ENSDF file for application purposes, are no longer stored on file but will be calculated individually upon user's request.

2. Catalog of Gamma Rays and Alpha Particles from Radioactive Decay (GAMCAT)

A Personal Computer version of a Catalog of Gammy Rays and of a Catalog of Alpha Particles has been created and is now available as a compact database. It is primarily designed for the use of scientists and technicians engaged in quantitative essay of radionuclides such as activation analysis, cross-section measurements, environmental pollution control, or waste composition control by means of gamma or alpha spectrometry. It should be a helpful tool in nuclear spectrometry where it can be used, for example, to identify gamma and alpha rays emitted from daugther nuclei or source impurities.

The database comprises three files:

* NUC:	nuclide file	2,587 nuclides
* GAM:	gamma ray file	46,950 gammas
* ALP:	alpha particle file	1,904 alpha lines

The file NUC contains information on radioactive and stable nuclides, such as spin, half-life,decay modes, or abundances. Comments and literature sources are also stored in file NUC. File GAM is a comprehensive collection of energies and emission probabilities of gamma and X-ray lines, while ALP is the corresponding file for alpha particles. Searching is possible in each of the three files. After finding a dataset in one file, the corresponding data of the other files can be displayed.

A convenient retrieval system has been developed for IBM AT computers or compatibles [2]. The Personal Computer is admirably suited for the presentation and handling of small to medium size collections of numeric or textual data. The more modern PCs running at processor speeds of 16 MHz or more surpass mainframe machines of only a few years ago in pure computing power. PC and Workstation software has set standards in terms of user friendliness which their mainframe counterparts with non-intelligent terminals fail to reach. A PC database is as readily available as a book and provides easier access to individual data than the printed version.

Attempts to implement GAMCAT with some of the commercial database systems on Personal Computers were quite unsatisfactory. Since most of these systems accept fixed lengths records only with predefined field sizes, a lot of space was wasted. Both data and index files were much larger than was really needed, which resulted in comparatively poor performance in terms of disk accesses for display and retrieval of data. Most commercial database systems provide for easy updating and addition of data and often use BTREE/ISAM accessing techniques. The overhead required for this is considerable and unnecessary in our case. The present data are essentially static and periodic updates can be handled by regenerating all of the files.
For these reasons a completely new system was written in C language and tuned to the particular problem at hand. Using data compression and encrypting, the elimination of sequences of blanks, and variable length records, space requirements were down by a factor of 10, from over 10 MB to 1.2 MB.

Retrieval is possible either by nuclear or by gamma or alpha energy. A data entry panel may be used (fullscreen mode) or retrieval commands (line mode). Also browsing in the gamma or alpha lines is possible. If a line is identified, it can be tagged and the full information on the parent decay may be shown.

GAMCAT is available on two HD floppy disks (either 3 1/2" or 5 1/4") from the Fachinformationszentrum (charged). The system runs on an AT-compatible computer with hard disk and 640 K byte of memory, operating under DOS 2.11 or later. 2 M byte of storage are needed on the hard disk.

3.) References:

1.) Nuclear Data Sheets for A=89
H. Sievers
Nuclear Data Sheets 56, 551 (1989)

2.) GAMCAT - A Personal Computer Database on Alpha Particles and Gamma Rays from Radioactive Decay
J.W. Tepel and H.-W. Müller
Nuclear Instruments and Methods, A286, 443 (1990)

APPENDIX

Addresses of Contributing Laboratories

Institut für Kernphysik III
Director: Prof. Dr. G. Schatz
Senior reporter: Dr. F. Käppeler
Kernforschungszentrum Karlsruhe
Postfach 3640
7500 Karlsruhe

Institut für Material- und Festkörperforschung II
Director: Dr. K. Anderko
Senior reporter: Dr. S. Cierjacks
Kernforschungszentrum Karlsruhe
Postfach 3640
7500 Karlsruhe

Institut für Neutronenphysik und Reaktortechnik
Director: Prof. Dr. G. Kessler
Senior reporter: Dr. F. Fröhner
Kernforschungszentrum Karlsruhe
Postfach 3640
7500 Karlsruhe

Institut für Chemie (1): Nuklearchemie
Director: Prof. Dr. G. Stöcklin
Senior reporter: Dr. S.M. Qaim
Forschungszentrum Jülich
Postfach 1913
5170 Jülich

Institut für Kernphysik,
Arbeitsgruppe Strahlungstransport
Head and senior reporter: Dr. D. Filges
Forschungszentrum Jülich
Postfach 1913
5170 Jülich

Institut für Kernphysik,
Experimentelle Kernphysik II
Director: Prof. Dr. O. Schult
Senior reporter: Prof. Dr. K. Sistemich
Forschungszentrum Jülich
Postfach 1913
5170 Jülich

Institut für Physik
Director: Prof. Dr. W. Michaelis
Senior reporter: Dr. R. Pepelnik
GKSS-Forschungszentrum Geesthacht GMBH
Postfach 1160
2054 Geesthacht

Zentraleinrichtung für Strahlenschutz
Head and senior reporter: Prof. Dr. H. Michel
Universität Hannover
Am Kleinen Felde 30
3000 Hannover 1

Abteilung Nuklearchemie
Director: Prof. Dr. G. Stöcklin
Senior reporter: Dr. U. Herpers
Universität zu Köln
Zülpicher Str. 47
5000 Köln 1

Institut für Kernchemie
Director: Prof. Dr. G. Herrmann
Senior reporter: Prof. Dr. H.O. Denschlag
Universität Mainz
Fritz-Strassmann-Weg 2
6500 Mainz

Fachbereich Physik der
Technischen Universität München
Abteilung E14, Forschungsreaktor
Senior reporter: Dr. W. Waschkowski
8046 Garching/München

Institut für Strahlenphysik
Director: Prof. Dr. C. Rolfs
Senior reporter: Dr J.W. Hammer
Universität Stuttgart
Allmandring 3
7000 Stuttgart 80

Physikalisch-Technische Bundesanstalt
Abteilung 6, Atomphysik
Director: Prof. Dr. R. Jahr
Bundesallee 100
3300 Braunschweig

Fachinformationszentrum Energie, Physik, Mathematik
Directors: Dr. W. Rittberger, E.-O. Schulze
Senior reporter: Dr. H. Behrens
Kernforschungszentrum
7514 Eggenstein-Leopoldshafen